

RESEARCH PAPER RP1221

Part of *Journal of Research of the National Bureau of Standards*, Volume 23,
July 1939

RATE OF OXIDATION OF STEELS AS DETERMINED FROM INTERFERENCE COLORS OF OXIDE FILMS

By Dunlap J. McAdam, Jr., and Glenn W. Geil

ABSTRACT

By use of interference colors, investigation has been made of the variation of thickness of the oxide film on steels with temperature and time. The rate of oxidation varies as a high power of the absolute temperature. If, over short intervals, the oxidation time at constant temperature is assumed to vary as a power of the film thickness, the exponent decreases from 100 or more for thin films to about 2 for thick films.

The film thickness, for constant oxidation time, increases rapidly with the absolute temperature. If, over short intervals, the thickness is assumed to vary as a power of the absolute temperature, the exponent increases with increase in film thickness, from 1 or less to about 20 or 25. The accelerating influence of temperature thus predominates over the retarding influence of increase in film thickness.

Various steels are compared, with reference to resistance to oxidation, and the influence of alloying elements is discussed.

CONTENTS

	Page
I. Introduction.....	64
II. Review of literature on the variation of the thickness of the oxide layer with temperature and time.....	67
1. Variation of film thickness with time, at constant temperature.....	67
2. Influence of temperature on oxidation time, for constant film thickness.....	69
3. Variation of film thickness with temperature, for constant oxidation time.....	70
III. Materials and methods.....	72
IV. Influence of temperature on oxidation time, for constant film thickness.....	73
1. General description of diagrams.....	73
2. Iron and carbon steels.....	75
3. Alloy tool steels and nickel steels.....	76
4. Chromium steels.....	76
5. Chromium-silicon and chromium-nickel steels.....	79
6. An equation to represent the influence of temperature on oxidation time, for constant film thickness.....	81
V. Variation of film thickness with time, at constant temperature.....	82
1. Derivation of diagrams.....	82
2. General description of diagrams.....	84
3. Form of the curves of variation of film thickness with time, at constant temperature.....	85
4. Comparison of typical diagrams.....	87
VI. Variation of film thickness with temperature, for constant oxidation time.....	90
1. General description of diagrams.....	90
2. Form of the curves of variation of film thickness with temperature, for constant oxidation time.....	90
3. Comparison of typical diagrams, representing the variation of film thickness with temperature.....	92
VII. Summary.....	92
VIII. References.....	93

I. INTRODUCTION

The practical importance of the resistance of metals to oxidation at elevated temperatures has led to various investigations of the rate of oxidation as affected by composition, temperature, and film thickness. In most of these investigations, the temperatures have been relatively high; oxidation, therefore, has been rapid and the oxide layers have been so thick that they should be considered as scales rather than as films. A few investigations have been made with slower rates of oxidation, and with oxide films thin enough to cause interference colors. As a study of thin continuous films appeared to be well adapted to give information of theoretical as well as practical importance, this method was chosen for the investigation herewith described. This investigation, therefore, has involved a study, by means of interference colors, of the rates of formation of thin continuous oxide films.

Interference colors do not appear until the film thickness reaches about 3×10^{-6} cm. The first stage of film formation is invisible to ordinary observation. A polarimetric study of the light reflected from the metal, however, reveals the presence of a film and gives a means of determining its thickness. At ordinary temperatures, in absence of moisture, oxide films on many metals do not increase in thickness beyond the invisible stage. On most metals at elevated temperatures and on some metals at room temperature, however, the films increase in thickness until eventually they cause interference colors.

These colors, sometimes called "temper" colors or "heat" colors, are caused by interference between rays of light reflected from the inner and outer surfaces of the oxide film. The coincidence of two waves differing in phase by 180° causes light of a certain wave length to disappear; if the incident light is "white," therefore, the reflected light is of the corresponding complementary color. Interference occurs when the film thickness is an odd multiple¹ of one-fourth the wave length of a component of the incident light. Interference, however, is determined by the wave length in the oxide film, not by the wave length in air. As the wave length in the film depends on the index of refraction of the oxide, the index of refraction is a factor involved in the relationship between wave length, film thickness, and interference color.

In this paper, attention is confined to oxidation of metals in the absence of liquid moisture. Oxidation of metals in air or oxygen at temperatures above the dew point was formerly considered to be a process of direct chemical combination, thus distinguished from ordinary corrosion. However, the investigations of Joffé and co-workers [15]² on electrical conductivity of dielectrics, and the later investigations of Wagner and coworkers [40, 25] on diffusion of metal ions, oxygen ions, and electrons through the oxide film, have shown that the oxidation of metals, even in the absence of moisture, is an electrochemical process.

The behavior of a metal in contact with air or oxygen is greatly influenced by temperature, and by the dissociation pressure of the oxide. The dissociation pressure, which varies with the temperature,

¹ The colors corresponding to multiples 1, 3, and 5 are known as colors of the first, second, and third order, respectively.

² Figures in brackets indicate the literature references at the end of this paper.

is the pressure of oxygen in equilibrium with the metal and its oxide. When the pressure of oxygen is less than the dissociation pressure, oxide does not form, and any oxide already formed decomposes. Oxides of "noble" metals have dissociation pressures greater than the partial pressure of oxygen in air. Oxides of base metals, however, have very low dissociation pressures at room temperature. The dissociation pressure of Cu_2O at 225°C , for example, is only 0.56×10^{-30} atmosphere; even at $1,725^\circ\text{C}$, the dissociation pressure is only 0.44 atmosphere. In air at atmospheric pressure, therefore, such metals tend to form oxide films even at room temperature.

The rate of oxidation of metals in air or oxygen depends not only on the composition, but also on temperature, and on the concentration (pressure) of oxygen in the gaseous phase. The rate of oxidation of most metals, moreover, varies with the thickness of the oxide layer. The thickness of this layer, however, has no appreciable effect on the rate of oxidation of some metals. This difference in behavior, as shown by Pilling and Bedworth [22], depends on the relationship between the volume of the oxide and the volume of metal from which the oxide was formed. When the volume of the oxide is less than the corresponding volume of metal, the oxide generally is porous, and thus does not prevent direct access of oxygen to the metal. As the rate of oxidation of such a metal (at constant temperature) is practically unaffected by the thickness of the layer of oxide, the thickness of this layer increases uniformly with time. When the volume of the oxide is greater than the volume of the metal from which the oxide is formed, the oxide film is under lateral pressure and tends to be nonporous. Such a film prevents direct access of oxygen to the underlying metal. To reach the metal, oxygen must enter the film and traverse it by diffusion [15, 40, 25]. The rate of oxidation, consequently, decreases with increase in the film thickness. In the first group of metals are most of the light metals, excepting aluminum. In the second group, which includes all other metals, are most of the metals in common use.

In the investigation described in this paper, attention was confined to rates of oxidation of steel in air at atmospheric pressure. The partial pressure of the oxygen surrounding the metal, therefore, varied only slightly. The concentration of the oxygen, however, obviously varied inversely with the absolute temperature used in an experiment. As the concentration of an element or compound taking part in a chemical reaction may greatly affect the velocity of reaction, consideration must now be given to the importance of the variable oxygen concentration.

The effect of oxygen concentration on the rate of oxidation has not been thoroughly investigated. Variation of the rate of oxidation with the pressure of oxygen, however, apparently is slight for all pressures above the dissociation pressure. Results of the investigation of oxidation of steels [22, 34, 35] at 800° to $1,100^\circ\text{C}$ appear to indicate that the rate of oxidation is about twice as great in oxygen as in air. If the variation is assumed to follow a power law, this would indicate that the average rate of oxidation varies as about the two-fifths power of the oxygen concentration. For copper [41] and nickel [41] at about $1,000^\circ\text{C}$, however, the oxidation rate was reported to vary as the seventh and sixth roots of the oxygen concentration. At these high temperatures, conditions were such that the oxide layers

were relatively thick; they were scales rather than continuous films. Investigations with steel at lower temperatures [27, 31] with films thin enough to cause interference colors, led the investigators to the view that variation of oxygen pressure between about 0.5 mm (of mercury) and atmospheric pressure has no discernible effect on the rate of oxidation. Oxygen concentration has also been reported to have no discernible effect on the rate of oxidation of zinc at 400° C [41]. The available evidence thus appears to indicate that the rate of oxidation in air is not appreciably affected by variation in oxygen concentration due to variation in temperature.

In the investigation described in this paper, the extreme temperature range for any one graph was sufficient to cause only about 50-percent variation in oxygen concentration. For an entire temperature-time-thickness diagram, however, the extreme range of oxygen concentration was sometimes as high as 3 to 1. Nevertheless, as the oxidation rate probably varied only as a small fractional power of the oxygen concentration, the effect of even the extreme range of oxygen concentration on the form of the diagram probably was small in comparison with the effects of temperature and film thickness.

The effect of water vapor in air or in oxygen, on the rate of oxidation, probably is negligible. Pilling and Bedworth [22] compared the effects of dry oxygen and of oxygen saturated with water vapor, on the rate of oxidation of copper; they found no discernible influence of the water vapor. Evans [6], in discussing the paper of Pilling and Bedworth, said that he had found dehydration of air to have no important effect on the rate of oxidation of iron. The rate of oxidation of metals in air at temperatures above the dew point, therefore, probably is not appreciably affected by variations in humidity.

The rate of oxidation of a metal may be expressed in terms of the rate of increase of film thickness with time. The rate of oxidation is not easily measurable; it is more convenient to measure the time interval from the beginning of exposure of the specimen to the attainment of any specified thickness. This time interval will be termed the oxidation time. (The mean rate of oxidation for this time interval is inversely proportional to the oxidation time.) The important factors to be considered in a study of the rates of oxidation of a given metal, therefore, are temperature, oxidation time, and film thickness. The thickness of the oxide layer has been investigated by a number of methods. In these methods, the variables observed (as indices of variation of film thickness) have included the weight change; the amount of oxygen combining with the metal; the change in electrical conductivity of the specimen; the quantity of electricity used in the reduction of the oxide film; and interference colors. To give a complete picture for any metal, however, such investigation should consider the interrelationship between all three important variables—temperature, oxidation time, and film thickness. Far-reaching conclusions have been formed and generally accepted, as a result of investigation of the relationship between only two of the variables throughout a narrow range of values. Such conclusions, as will be seen, may not be generally correct.

In obtaining a three-dimensional picture for any metal, it is necessary to obtain three complementary views, each based on a study of the relationship between two of the variables, with the third variable held constant. One of these two-dimensional views is based on

the relationship between temperature and time for constant interference color (constant film thickness). Results of such an investigation are given in Section IV. Another two-dimensional view has been obtained by investigating the relationship between oxidation time and film thickness (as determined from the entire range of temper colors), with temperature held constant. Results of this investigation are given in section V. From any pair of these views, it is possible to derive a third view, representing the relationship between temperature and film thickness, for constant oxidation time. Diagrams representing this relationship are discussed in section VI.

II. REVIEW OF LITERATURE ON THE VARIATION OF THE THICKNESS OF THE OXIDE LAYER WITH TEMPERATURE AND TIME

1. VARIATION OF FILM THICKNESS WITH TIME, AT CONSTANT TEMPERATURE

In discussing the literature dealing with the relationship between temperature, time, and film thickness, it is convenient to consider successively all the two-dimensional views of this three-dimensional relationship. These views represent the variation of film thickness with time at constant temperature; the influence of temperature on oxidation time, for constant film thickness; and the variation of film thickness with temperature, for constant oxidation time. The first of these two-dimensional views will now be considered.

When the volume of an oxide is greater than the volume of the metal from which it is formed, the rate of oxidation decreases with increase in the thickness of the oxide film. The oxidation time, therefore, increases more than in proportion to the film thickness. Several equations have been suggested to represent this variation of film thickness with time. The most widely accepted of these equations is based on theoretical considerations, which were stated first by Pilling and Bedworth [22]. According to this theory, the rate of oxidation depends on the steepness of the concentration gradient of oxygen between the outer and inner surfaces of the film. At the inner surface the equilibrium concentration would be about that corresponding to the dissociation pressure of the oxide in contact with the metal. At the outer surface of the film, the equilibrium concentration of dissolved oxygen would be the saturation value at that temperature. On the tacit assumption that the range of oxygen concentration is constant, the theory would imply that the steepness of the gradient, and hence the instantaneous rate of oxidation, varies inversely as the film thickness. The equation representing this relationship, for constant temperature, is

$$dy/dt = K/y \quad (1)$$

In this equation, y represents film thickness, t represents time, and K is a constant. Integration of this equation gives the equation for a quadratic parabola

$$y^2 = 2Kt + C \quad (2)$$

In this equation, C is a constant of integration and represents the square of the initial film thickness.

According to this theory, therefore, the film thickness (at constant temperature) increases as the square root of the time, if the time is

measured from the instant that the thickness is zero. Experimental investigation by Pilling and Bedworth [22] led them to the view that the results substantiated the theory, which they thereafter called the "quadratic law." Numerous other investigators [5, 12, 14, 16, 21, 23, 24, 26, 29, 34, 35, 36, 37, 38, 39, 42] have reported that their results substantiate this relationship, which has been frequently called the "parabolic law." In all these investigations, however, temperatures were relatively high and oxidation times were sufficient to cause relatively thick scale. Experiments with thinner layers of oxide have led some investigators to report deviations from the parabolic relationship. Such deviations in the early stages of oxidation were reported by Portevin, Prétet, and Jolivet [23, 24] and by Feitknecht [10], as a result of their investigations with electrolytic iron and copper, respectively. Vernon [39] reported that the oxidation of iron did not conform to the parabolic relationship at temperatures below 200° C. An investigation of single crystals of low-carbon iron by means of interference colors led Mehl and McCandless [17] to the view that the oxidation did not conform to the parabolic relationship. Miley [18] and Miley and Evans [19], as a result of electrometric studies of oxide films, reported that the oxidation of iron and copper (at 350° C and below) did not conform to the parabolic relationship, except for a short initial period of heating. Their conclusions thus appear to be the opposite of those reached by several investigators previously mentioned. As shown in section V, the apparently contradictory views reached by investigators of this subject are due largely to the attempt to draw general conclusions from too narrow ranges of the variables.

A very different representation of the variation of film thickness with time was obtained by Tammann and coworkers [27, 31, 32]. By use of interference colors they investigated the oxidation of iron, copper, nickel, zinc, cadmium, tin, lead, cobalt, and manganese. They reported that the variation of film thickness with time was in accordance with an exponential equation

$$t = ae^{bv} - a \quad (3)$$

In this equation, t and y have the same significance as in eq 1 and 2, and the other letters represent constants. One of these constants, a , was said to be independent of temperature; the other constant, b , was said to be dependent on temperature in accordance with another exponential equation. In developing eq 3, however, Tammann and Koster assumed that the film thickness for second-order colors is only twice the thickness for first-order colors. As pointed out by Evans [7] and Dunn [4], this assumption is incorrect, and the equation of Tammann and Koster is not in accordance with the data. In a later paper, Tammann and Bochow [30] reported that the exponential relationship was followed exactly in the oxidation of nickel, but not exactly in the oxidation of copper. They did not indicate, however, whether or not their calculations were based on their original incorrect assumption as to the relationship between interference colors and film thickness. Confirmation of the Tammann and Koster exponential equation was reported by Schwarze [28], who used interference colors in studying the oxidation of fourteen steels in the temperature range 300° to 380° C.

An exponential relationship and a parabolic relationship could not both be correct as a general representation of the variation of film

thickness with time. As shown in section V, these relationships are not generally correct, nor is any other single formula generally correct.

2. INFLUENCE OF TEMPERATURE ON OXIDATION TIME, FOR CONSTANT FILM THICKNESS

Very few investigators have studied the variation of oxidation time or of its reciprocal, the mean oxidation rate, with temperature, for constant film thickness. In most investigations of oxidation of metals at elevated temperatures, increases of weight (or other indices of film thickness) have been compared, for constant oxidation time. Results of such investigations are considered in section II (3).

A study of the influence of temperature on the oxidation time, for constant film thickness, may be readily made by means of interference colors. Constancy of interference color, for the same metal, means approximate constancy of film thickness. The previously mentioned investigations of Tamman and coworkers dealt with the relationship between film thickness and both time and temperature. In their exponential equation representing the variation of film thickness with time, constant b was said to vary with temperature in accordance with another exponential equation. Although their equations were based on an incorrect assumption as to the relationship between film thickness and interference colors, Schwarze [28] reported that both equations were substantiated by results of his investigation. Entirely different equations have been reported by other investigators.

In practically all other investigations, however, much higher temperatures were used, and the oxide layers were from ten to a thousand times as thick as those obtained in investigations by means of interference colors. As a result of an investigation of this kind, Pilling and Bedworth [22] suggested the equation

$$K = aT^n \quad (4)$$

In this equation, T represents absolute temperature, K is an "oxidation rate constant", and a and n are other constants. The oxidation rate represented by K is neither the instantaneous rate, dependent on film thickness, nor the average rate. It is derived from eq 1, based on the previously mentioned theory of Pilling and Bedworth. According to this theory, the "rate constant", K , is independent of film thickness and is characteristic of the metal at the given temperature. As shown in section V, however, the relationship represented by eq 1 is not generally correct, although it may be approximately correct as applied to relatively thick, rapidly formed oxide layers.

In a theoretical discussion of the influence of temperature on the oxidation rate, Dunn [5] reasoned that the rate of oxidation is determined by the rate of diffusion through the oxide film, and that "an oxygen molecule can only pass a structural unit, provided that it possesses at the moment energy greater than a critical value causing a loosening of the oxide structure at that point." He thus arrived at the relation

$$K = Ae^{-b/T} \quad (5)$$

In this equation, T represents absolute temperature, K is the "oxidation rate constant" derived from eq 1, and A and b are constants. From this equation may be derived the equation

$$\log K = -b/T + \text{constant} \quad (6)$$

Dunn reported that results of his experiments with brasses in the temperature range 580° to 880° C., and also the results obtained by Pilling and Bedworth on the oxidation of copper, iron, and nickel, conform closely to this relationship.

The same equation was developed by Heindlhofer and Larsen [12] on reasoning (similar to that of Pilling and Bedworth) that the rate of oxidation depends on the concentration-gradient of dissolved oxygen and on the specific diffusivity of the oxygen in the oxide film. Their experimental results on the scaling of commercially pure iron between 600° and 1,100° C, and also pure copper between 600° and 1,100° C, were said to conform to this relationship. They concluded that the relationship is satisfactorily represented by eq 6, provided that the instantaneous rate of oxidation is not so high that it is affected by the rate of diffusion of oxygen in the gaseous phase, and provided that there is no blistering or discontinuity in the oxide layer. They also discussed the possible difference in diffusion in layers of different oxides of the same metal.

Confirmation of the exponential relationship represented by eq 5 and 6 has also been reported by Portevin, Prétet, and Jolivet [23, 24], as a result of their experiments with electrolytic iron in the temperature range 800° to 1,000° C. When $\log K$ was plotted against the reciprocal of the absolute temperature, they obtained two straight lines intersecting at an angle of nearly 180°, at about 900° C. They considered the apparent change of direction at this point to be due to the transition from alpha to gamma iron. With some allowance for scatter of experimental points, however, the relationship could be represented nearly as well by a single straight line, but could be represented even better by a slightly curved line. A practically straight line would be obtained also by plotting $\log K$ against $\log \bar{T}$, thus indicating a relationship similar to that shown (for much thinner films) in section IV.

Linear relationship between $\log K$ and $1/T$ has also been reported by Krupkowski and Jaszczurowski [16], as a result of their experiments with nickel and iron in the temperature range 500° to 1,200° C.

Hudson and Rooney [13], after studying the results obtained by previous investigators on the scaling of iron and carbon steels, concluded that the results conform equally well to eq 4, which gives a linear relationship with $\log K$ plotted against $\log T$, or to eq 5, which gives a linear relationship with $\log K$ plotted against $1/T$. All the results on which these conclusions were based, however, were obtained with relatively high rates of oxidation and with relatively thick layers of oxide. For slower rates and for thin films, the only formula hitherto available has been the previously mentioned complex exponential equation suggested by Tammann and coworkers [27, 31, 32]. As shown in section IV, this formula is not generally correct.

3. VARIATION OF FILM THICKNESS WITH TEMPERATURE, FOR CONSTANT OXIDATION TIME

A number of investigators have studied the variation of thickness of the oxide layer with temperature, for constant oxidation time. In most of these investigations, increase in weight has been used as a measure of the increase in thickness.

Dickenson [3] compared the increase in weight of various carbon steels and alloy steels, in 5 hours at various temperatures within the

range 550° to 1,100° C. Practically straight lines were said to be obtained by plotting the logarithms of the average oxidation rates (for the 5-hour period) against either the absolute temperatures or the logarithms of these temperatures. The latter relationship would give an equation of the same form as eq 4, developed by Pilling and Bedworth [22]. The two equations, however, do not involve the same variables. The equation derived from Dickenson's data represents the variation of the average rate of oxidation (increase of thickness), for constant time. The equation derived from the data of Pilling and Bedworth represents the influence of temperature on an "oxidation rate constant," assumed to be independent of thickness. Although the two equations could be of the same form, therefore, the derived constants representing the slopes of the straight lines (plotted with logarithmic coordinates) would be very different. As shown in section VI, however, an equation of this form is not a generally correct representation of the variation of thickness with temperature, for constant oxidation time.

A quite different relationship between film thickness and temperature has been reported by Hudson, Herbert, Ball, and Bucknall [14], and by Vernon [39]. Both investigations, the former with copper and the latter with iron, determined the gains in weight during 1 hour at various temperatures. Results of both investigations were said to indicate that the logarithm of the gain of weight (thickness) is proportional to the reciprocal of the absolute temperature. The equation representing this relationship, therefore, is similar in form to eq 6, developed by Dunn. In eq 6, however, one of the variables is an assumed "oxidation rate constant"; in the equation based on data of Hudson, Herbert, Ball, and Bucknall [14], the corresponding variable is the increase in thickness (weight) for constant oxidation time. Although the two equations could be of the same form, therefore, the derived constants would be very different. As shown in section VI, however, an equation of this form is not a generally correct representation of the variation of film thickness with temperature, for constant oxidation time.

A still different relationship has been reported by Rickett and Wood [26], who determined the gains in weight of some chromium steels (0 to 30 percent of chromium) for constant time at various temperatures. They reported a linear relationship between the logarithm of the gain in weight and the absolute temperature. An equation of this form, as shown in section VI, cannot be considered generally correct.

Murphy, Wood, and Jominy [21] have reported that the scaling of steel in the temperature range 1,093° to 1,315° C can be represented by a linear relationship between the gain in weight and the absolute temperature. Upthegrove and coworkers [29, 34, 35], who studied the scaling of SAE 1015 and 1020 steels in the temperature range 900° to 1,150° C found no simple relationship between oxidation and temperature. Graphs of weight change, for constant oxidation time, were said to show an abrupt change at 980° C for scaling in oxygen. For scaling in air, they reported a maximum and minimum at about 980° and 1,100° C, respectively.

The various investigations on this subject, therefore, have led to contradictory conclusions. As shown in sections IV, V, and VI, many of these apparent discrepancies probably are due to deductions based on narrow ranges of only two of the three important variables.

III. MATERIALS AND METHODS

The steels used in this investigation may be classified as follows: carbon steels; tool steels; nickel steels; steels containing up to 5 percent of chromium; high-chromium steels; chromium-silicon steels; medium-chromium, high-nickel steels; high-chromium steels containing nickel. The compositions of these steels are given in table 1.

The specimens used for heat coloring were about 1 cm² in area and 1 mm thick. One surface was polished by the method used for metallographic specimens. The most suitable method of polishing was determined by trying various grades of abrasive and various polishing methods. The most uniform and brilliant coloring was obtained with specimens that had been polished dry by a series of emery papers (Nos. 1G, 0, 00, and 000), and then polished wet with levigated alumina. Additional polishing with magnesium oxide produced no significant effect on the subsequent coloring. The specimens were washed in alcohol, then with carbon tetrachloride, and were allowed to dry in air. To avoid nonuniform coloring, the surface was not afterward touched. The specimens were kept in desiccators, at room temperature, until ready for use.

At temperatures above 220° C, heat coloring was done in a small electric resistance furnace of the muffle type. A chromel-alumel thermocouple was used for measuring temperatures. The temperature was maintained, by controllers of the automatic potentiometer type, within 0.5 percent of the desired absolute temperature. To provide slow continuous change of the air inside the furnace, and thus to prevent depletion of the supply of oxygen, the opening in the top of the furnace was kept only partially covered.

At temperatures of 220° C and less, heat coloring was done in small electric ovens with automatic temperature control. Air circulation was provided by a fan and by two small openings in the furnace, one in the top and one in the side near the bottom. No difference in results (at 200° C) however, was observed when the fan was not operating and when the openings were closed. Although the speed of air flow across the heated surface (as shown by Upthegrove [34] and others) affects the scaling rate at 1,000° C or higher, at lower temperatures the effect of ordinary variations in air velocity is small.

The specimens, with the polished surface upward, were placed in the furnaces and ovens on stainless-steel plates. Such a plate served two purposes; it increased the thermal capacity of the furnace and hence was an aid in keeping the temperature constant, and it hastened the approach of the temperature of the specimen to the temperature of the furnace. Some tests with a silver plate instead of the steel plate gave unsatisfactory results; the coloring rate, especially of steels with chromium present, was accelerated by contact with the silver, although the polished surface of the specimen was not in contact with the silver. Analysis of the colored oxide film gave no indication of silver or silver compounds. Use of silver, for supporting the specimens, however, was discontinued.

There is no sharp demarcation between succeeding colors in the interference color scale. The colors change through the following sequence: Straw color, light yellow or gold, golden brown, brown with reddish or purple tint, brownish purple, light purple, dark purple,

dark blue, light blue,³ very light greenish blue with a silvery gray appearance. The color sequence is then repeated with the colors less brilliant and less easily distinguishable.

The most easily distinguishable colors were selected for this time-temperature study. One of these is the first visible color, a very light straw color, another is brown with the first tinge of red or purple, and another is dark blue. The brown color could not be distinguished as sharply as the dark-blue color. The second-order colors selected were essentially the same. The colors of the second order were somewhat masked by the specific color of the oxide itself; on most of the specimens higher orders of color were not distinguishable.

For the tests at temperatures above 220° C, the coloring of the specimens was followed by frequent observation through the opening in the top of the furnace. For the tests at 220° C and below, observation of the coloring was made through the door of the oven, which was opened for each observation. Before inserting the specimen, the furnace or oven was allowed to attain the desired temperature. The oxidation time was reckoned from the instant the specimen was placed upon the steel plate. As about 1½ minutes' time was required for the specimen to attain the temperature of the oven, however, some correction was necessary in estimating the equivalent oxidation time at the desired temperature. This correction is important for short oxidation times, but usually unimportant for oxidation times greater than about 20 minutes.

The relationship between temperature, time, and film thickness has been studied by means of plan views, front views and side elevations of three-dimensional diagrams. Plan views, in which the coordinates represent temperature and oxidation time, are discussed in section IV. Front views, in which the coordinates represent time and temperature, are discussed in section V. Side elevations, in which the coordinates represent temperature and film thickness, are discussed in section VI.

IV. INFLUENCE OF TEMPERATURE ON OXIDATION TIME, FOR CONSTANT FILM THICKNESS

1. GENERAL DESCRIPTION OF DIAGRAMS

In a study of the variation of film thickness with temperature and time, the first relationship to be considered is the relationship between temperature and time, for constant film thickness (constant interference color). Diagrams (see footnote 4) representing this relationship for a variety of steels are shown in figures 1 to 15, inclusive, and diagrams comparing the results obtained with typical steels are shown in figures 16 to 19, inclusive. Each steel is designated by a letter, which is used also to identify it in the table of chemical compositions, table 1.

After trying various methods of plotting the results, logarithmic coordinates were chosen, because each graph⁴ so plotted was found to be practically straight throughout most of its length. Abscissas represent time in minutes; at the top of each figure is an additional scale representing days. As ordinates, an attempt was made to use

³ This is not in accordance with the statements of several investigators, who have reported that light blue appears before dark blue.

⁴ The word "graph" is used to designate a single representative straight line or curve. The word "diagram" is used to designate a series or family of graphs.

the first power of the absolute temperatures. The slopes of the graphs, however, were so slight that they could not be determined with sufficient accuracy. By plotting a power of the absolute temperature, as ordinates, it is possible to increase the slope of a graph (drawn with logarithmic coordinates) without distortion. In figures 1 to 19, ordinates represent the tenth power of the absolute temperatures. By this means, the slope (tangent of the angle) has been multiplied by 10. Each figure also contains a scale in degrees centigrade.

Preceding the series of diagrams is a general legend, giving the symbols and their significance. A special legend is also included in each figure.

In each diagram of figures 1 to 15, are graphs representing the temperature-time relationship for straw color, reddish brown, and blue. Two of the diagrams, figures 8 and 12, include only the graphs for colors of the first order. The other diagrams include graphs for colors of both the first and second order, and the diagrams of figures 1, 10, and 14 include also the graphs for third-order blue. Each line is designated by letter (*X*, *Y*, or *Z*) representing straw color, reddish brown, or blue, respectively. For second- and third-order colors, this letter is followed by a numeral (2 or 3) to designate the order of the color.

Second-order colors are less distinct than first-order colors, and third-order colors are much less distinct than second-order colors. The distinctness of the colors varies with the composition of the steel. The 5-percent-chromium steel and the 46-percent-nickel steel gave second-order colors too indistinct to be used in studying the influence of temperature and time on film thickness. The only materials that gave third-order colors distinct enough to be used were electrolytic iron, 24-percent-chromium steel, and 25:20 chromium-nickel steel. No fourth-order colors could be distinguished on any of the steels. The indistinctness of the second- and third-order colors probably is not due entirely to decrease in transparency of the film with increase in thickness, but is due largely to coincidence of different colors of different orders. Third-order straw color probably appears before second-order blue; second-order blue thus probably coincides with some third-order color between straw and reddish brown. Third-order blue probably coincides with different colors of the fourth and fifth orders.

The experimental points in these figures represent the observed total oxidation times, with no correction for the time required for heating the specimen to the temperature of the furnace, nor for the effect of temporary lowering of the temperature each time the furnace was opened to facilitate observation of the colors. The number of such observations for any one specimen, however, generally was relatively small, except for second- and third-order colors. Because of the indistinctness of second- and third-order colors, more frequent observations were necessary in order to determine the time at which such a color reached its maximum.

The time required for this rise of temperature of the specimen varied with the temperature of the furnace. The periods necessary to heat a specimen to 650°, 530°, 355°, and 220° C, were 1.57, 1.52, 1.47, and 1.44 minutes, respectively. As the time probably is nearly proportional to the logarithm of the range of temperature through which the specimen is heated, the time required for heating the speci-

men to a furnace temperature of 950° C, the highest temperature used on these experiments, probably was about 1.65 minutes. Correction of the observed oxidation time, therefore, evidently is important when the total time is less than about 20 minutes.

The solid-line graphs in figures 1 to 15 are based on the uncorrected positions of the experimental points. Each line is based not only on the experimental points belonging to that line, but also on the probable ideal interrelationship (in form and position) between all the lines of the diagram. In determining the form of such a diagram, moreover, consideration was given to the complementary diagrams of two other types, which are illustrated in figures 21 to 28, inclusive, and discussed in sections V and VI. Each diagram of the type shown in figures 1 to 15 thus represents a plan view of a three-dimensional diagram in which the graphs are contour lines.

2. IRON AND CARBON STEELS

Diagrams for iron and pearlitic carbon steels, ranging in carbon content from 0.008 to 1.29 percent, are shown in figures 1, 2, and 3. The experimentally determined parts of the diagrams extend to temperatures as low as 100° C.⁵ The solid lines representing the various interference colors are nearly straight throughout most of their extent, but are curved throughout the portions representing short oxidation time. These lines, however, are not corrected to allow for the time required to heat the specimen to the temperature of the furnace. The relative amount of such correction increases with decrease in the total oxidation time.

The lines representing the first-order colors, if correction were applied for the time of initial heating, evidently would become straight throughout the entire range of experiment. Such straightening is indicated by the broken lines diverging from some of the solid lines. The lines representing second- and third-order colors could be straightened only by applying a somewhat larger correction. A larger correction for these lines, however, is justifiable, because the indistinctness of the second- and third-order colors made it necessary to open the furnace frequently to examine the specimen. Complete correction of the oxidation time for second- and third-order colors, therefore, probably would straighten these lines throughout the entire represented range of time.

In all the diagrams of figures 1, 2, and 3, the slope is greatest for the line representing first-order straw color and is least for the highest⁶ line in each diagram. The slope, therefore, evidently decreases with increase in the corresponding film thickness; the corrected lines, consequently, converge toward the top of the diagram. The difference in slope between two adjacent lines moreover, evidently decreases with increase in the corresponding film thickness.

The relative heights of these and following diagrams may be determined by comparing not only the figures containing the entire diagrams, but also by comparing corresponding single lines reproduced and assembled in figures 16 to 19. Each of these figures contains lines representing the same interference color for various steels.

⁵ This is not in accordance with results reported by Vernon [39] and by Miley and Evans [20], who stated that interference colors could not be obtained below 200° C.

⁶ The higher of two points in the two-dimensional diagram is the point whose ordinate is greatest.

The diagrams in figures 1, 2, and 3 differ little in position. The diagrams for 0.46-percent-carbon steel, *D*, and 0.83-percent-carbon steel, *E*, however, are somewhat higher than the diagrams for steels of either lower or higher carbon content, with the exception of the lines representing first-order straw color. This relationship is illustrated in figures 16 to 19 by the relative positions of line *A*, representing electrolytic iron, and line *E*, representing 0.83-percent-carbon steel. For first-order straw color, as shown in figure 16, lines *A* and *E* coincide. For the other interference colors, as shown in figures 17, 18, and 19, line *E* is above line *A*. At the right end, the difference in height is small, but the difference increases as the lines extend to the left.

The steels represented in figures 1, 2, and 3 are pearlitic steels. Consideration was given, however, to the influence of variation of microstructure due to heat treatment. Specimens of the 0.83-percent-carbon steel were heated to 1,450° F and cooled at various rates. Some specimens were quenched in water, others were cooled in air, and others in the furnace. Although these differences in heat treatment caused great differences in microstructure, the specimens showed no significant differences in the temperature-time relationship for interference colors.

3. ALLOY TOOL STEELS AND NICKEL STEELS

The diagrams representing alloy steels, in figures 4 to 15, are qualitatively similar to the diagrams for carbon steels. The corrected graphs are approximately straight, and the lines in each diagram diverge as they extend to the right. The divergence, however, is greater in some diagrams than in others, and the lines in some diagrams are generally steeper than in others. The relative heights and widths (range of coordinates) of the diagrams, moreover, are influenced by the alloying elements.

In figures 4 and 5 are typical diagrams for alloy tool steels, one of them a high-speed steel. In form and position these diagrams do not differ appreciably from the diagrams for carbon steels. Neither the small percentages of alloying elements in steels *G* and *H* nor the larger percentage of chromium and the large percentage of tungsten in high-speed steel have had any apparent effect on the height of the diagram.

In figure 6 are diagrams representing two nickel steels. The diagram for 3.35-percent-nickel steel, *J*, almost coincides with the diagram for 0.83-percent-carbon steel, *E*. The diagram for the 32-percent-nickel steel, *K* (as shown in figs. 16 to 19, inclusive) is somewhat higher than the diagrams for carbon steels. The large percentage of nickel in steel *K*, in absence of chromium, apparently had little effect in increasing the resistance of steel to oxidation.

4. CHROMIUM STEELS

In figures 7 to 10 are diagrams representing chromium steels, with percentages of chromium ranging between 1.38 and 24.4. The diagrams in figure 7 represent steels with small percentages of chromium. The width (vertical range) of each of these diagrams is greater than the width of a diagram representing carbon steel. This is illustrated, in each of the diagrams of figures 16 to 19, by the

relative position of line *M*, representing 2.18-percent-chromium steel. (Lines for the 1.38-percent-chromium steel, *L*, if drawn in these diagrams, would practically coincide with line *M*).

For first-order straw color (fig. 16), line *M* is below the lines (*A* and *E*) representing carbon steels. For first-order brown and blue (figs. 17 and 18), line *M* is between lines *A* and *E*. For second-order blue (fig. 19), line *M* is considerably above the lines representing carbon steels. Resistance to oxidation of steels with small percentages of chromium, therefore, evidently is less than that of carbon steels until the film thickness exceeds a value corresponding to first-order straw color. With further increase in film thickness, the apparent accelerating effect of the chromium on oxidation wanes; a retarding effect begins when the film thickness reaches a value corresponding to some second-order color.

In figure 8 the diagram for steel *N*, represented by the solid lines, shows the influence of about 5 percent of chromium. The second-order colors obtained with this steel were too indistinct to be used to establish lines. For the first-order colors, the experimental points show little scatter and the lines appear to be well established. The width of the first-order portion of the diagram for this steel is much greater than the widths of the corresponding portions of the diagrams representing carbon steels and low-chromium steels. This portion of the diagram for 5-percent-chromium steel extends below and above the corresponding portions of the diagrams for the steels previously discussed. For first-order straw color (fig. 16), line *N*, representing 5-percent-chromium steel, is below the lines representing carbon steels. For a large part of its length, moreover, line *N* is below line *M*, representing 2.18-percent-chromium steel. For first-order brown (fig. 17), line *N* is above line *M*, and (throughout most of its length) is above line *E*, representing 0.83-percent-carbon steel. For first-order blue (fig. 18), line *N* is considerably above line *E*, and almost coincides with line *K*, representing 32-percent-nickel steel. If lines could be established to represent second-order colors, they probably would show still further improvement in relative height of the diagram for 5-percent-chromium steel, corresponding with the further increase in film thickness.

The influence of 5 percent of chromium evidently is qualitatively similar to the previously described influence of smaller percentages of chromium. Resistance to oxidation is less for these steels than for carbon steels until the film thickness exceeds a value corresponding to first-order straw color. With further increase in film thickness, the apparent accelerating effect of chromium on oxidation disappears; a retarding effect then begins and increases with further increase in film thickness, at least to values corresponding to second-order colors.

In figure 9 is a diagram representing 13.6-percent-chromium steel. The scatter of experimental points is such that this diagram is less exactly established than are the diagrams previously described. The line for first-order brown may be somewhat too low. The lines, moreover, possibly should diverge more as they extend to the right. The diagram as drawn to represent the probable interrelationship of the lines, however, is considered approximately correct.

The curvature of the uncorrected upper lines in this figure extends further to the right than in any of the diagrams previously described. The greater extent of the curvature probably is connected with the

range of relatively high temperature represented by the upper part of this diagram. Whereas no diagram previously described extends above about 450° C, this diagram extends to 950° C. The curved portions of the lines representing second- and third-order colors, therefore, are based on observations with the specimen at red heat. To observe the interference colors, it was necessary either to remove these specimens from the furnace long enough for the temperature to drop below red heat, or to observe the colors by reflected light, with the specimen at red heat. The former procedure would necessitate a relatively large correction to allow for the times of repeated cooling and reheating. The latter procedure, which was generally used, caused mixture of the interference color with the red light emanating from the specimen. The admixture of red would tend to delay the observed appearance of second- and third-order blue, and thus would tend to increase the curvature of the corresponding lines. Complete correction of these lines, therefore, probably would make them practically straight.

The width of this diagram is about twice as great as the width of the diagrams for carbon steels. As shown in figure 8 (in which the lines for the 13.6-percent-chromium steel are reproduced for comparison), moreover, the diagram for 13.6-percent-chromium steel is much wider than the diagram for the 5-percent-chromium steel. The lower limit of the diagram for 13.6-percent-chromium steel, however, is above the lower limit of the diagram for 5-percent-chromium steel. Whereas chromium in percentages up to at least 5 evidently tends to lower the line representing first-order straw color, 13.6 percent of chromium raises this line considerably.

The beneficial effect of 13.6 percent of chromium evidently increases with increase in the film thickness, at least up to values represented by second-order blue. This is illustrated by the relative position of line *O* in figures 16 to 19, inclusive. For film thicknesses corresponding to first- and second-order blue, as shown in figures 18 and 19, line *O* is in the group of lines representing alloys with high resistance to oxidation.

In figure 10 is a diagram for steel *P* containing 24.4 percent of chromium. The width of this diagram is somewhat less than the width of the diagram representing 13.6-percent-chromium steel. The smaller width of the diagram for 24.4-percent chromium steel, however, is due almost entirely to the relatively high positions of the lines representing first-order straw color and brown. The line representing first-order straw color, as shown in figure 16, is considerably higher for the 24.4-percent-chromium steel than for the 13.6-percent-chromium steel. In figure 17, line *P* is far above line *O*. As previously stated, however, line *O* may be slightly too low. In figure 18, line *P* is slightly higher than line *O*. For second-order blue (fig. 19), however, line *P* is slightly below line *O*. In view of the previously mentioned uncertainty as to the exact position of some of the lines representing the 13.6-percent-chromium steel, it appears probable that the upper boundaries of the diagrams for 13.6- and 24.4-percent-chromium steels practically coincide.

The beneficial influence of increase in the chromium content beyond about 13 percent, therefore, applies chiefly to the initial stage of oxidation, represented by the growth of the film to a thickness

corresponding to first-order blue. In this stage, 24-percent-chromium steel appears to be definitely superior to 13-percent-chromium steel.

5. CHROMIUM-SILICON AND CHROMIUM-NICKEL STEELS

In figure 11 is a diagram representing steel *Q*, containing 8.8 percent of chromium and 2.8 percent of silicon. The uppermost line of this diagram is in about the same position as the corresponding lines representing 13.6- and 24.4-percent-chromium steels. The line representing first-order straw color (line *Q* of fig. 16), however, is far below the corresponding lines representing 13.6- and 24.4-percent-chromium steels, and is about as low as the lines representing 2.18- and 5-percent-chromium steels. The vertical range of the diagram for steel *Q* thus spans the vertical ranges of all the other diagrams investigated.

With increase in the film thickness from a value represented by first-order straw color to a value represented by first-order brown, the relative position of line *Q* (figs. 16 and 17) is greatly improved; line *Q* is thus raised above line *O*, representing 13.6-percent-chromium steel. With further increase in film thickness to values represented by first- and second-order blue, the relative position of line *Q* is still further improved. For first-order blue, line *Q* almost coincides with line *P*, representing 24.4-percent-chromium steel; for second-order blue, line *Q* is slightly above line *P*.

Resistance to oxidation of the steel containing 8.8 percent of chromium and 2.8 percent of silicon, therefore, was inferior to the resistance of steel containing 13.6 percent of chromium until the film thickness exceeded a value corresponding to the first interference colors. With further increase in film thickness, the resistance of the chromium-silicon steel became superior to that of the 13.6-percent-chromium steel.

In figure 12 is a diagram representing steel *R*, containing 8.8 percent of chromium, 46.8 percent of nickel, 3.6 percent of cobalt, and 1.5 percent of silicon. The steel was made at this Bureau some years ago for use in experiments on creep of metals at elevated temperatures. In its effect on resistance to oxidation, the 3.6-percent of cobalt (in steel of this composition) probably is about equivalent to the same percentage of nickel. The resistance of this steel to oxidation, therefore, probably is about that of a steel containing 8.8 percent of chromium, 1.5 percent of silicon, and about 50 percent of nickel.

The line representing first-order straw color, if plotted in figure 16, would almost coincide with line *M*, representing 5-percent-chromium steel; it would thus be below the lines representing carbon steels. The lines for brown and blue in figure 12 are unusually steep. The line for brown, if plotted in figure 17, would be between lines *E* and *K* at the right end and between lines *K* and *O* at the left end. It would thus be far above the lines for carbon steels. The line for first-order blue, if plotted in figure 18, would be considerably above the lower group of lines, but far below the line for 13.6-percent-chromium steel and the line for the steel containing 8.8 percent of chromium and 2.8 percent of silicon. The second-order colors were too indistinct to be used in establishing lines.

Steel *R*, therefore, has much less resistance to oxidation than steel *Q*, which has the same percentage of chromium but no nickel. The large amount of nickel in steel *R*, in conjunction with the 8.8 percent

of chromium, evidently was less effective in retarding oxidation, than the 2.8 percent of silicon in steel *Q*. Comparison of the diagram for steel *R* with the diagram (fig. 6) for steel *K*, containing 32 percent of nickel but no chromium, indicates that the 8.8 percent of chromium in steel *R* had considerable effect in increasing resistance to oxidation.

In figures 13 and 14 are diagrams representing two chromium-nickel steels with high percentages of chromium. The diagram (fig. 13) for steel *S*, containing 18.2 percent of chromium and 8.6 percent of nickel, differs little in form and position from the diagram for the 24.4-percent-chromium steel, *P* (fig. 10). The lines representing first-order colors in the two diagrams are at about the same height at the right end; at the left end, the line for first-order straw color is lower for steel *S* than for steel *P*. The lines for first-order brown and blue, however, are higher for steel *S* than for steel *P*. The lines representing second-order colors are higher, throughout their whole extent, for steel *S* than for steel *P*. The rates of oxidation of the two alloys, therefore, were at first about the same. With increasing film thickness, however, the rate of oxidation became less for the 18:8 chromium-nickel steel than for the 24.4-percent-chromium steel.

The diagram for the 25:20 chromium-nickel steel, *T*, (fig. 14), is lower than the diagram for the 18:8 chromium-nickel steel, *S*, except at the lower boundary and the upper-right corner. The lines for first-order straw color in the two diagrams, in view of the scatter of experimental points in figure 13, show no significant difference in height. The lines for first-order brown and blue and for second-order straw color, however, are distinctly lower for steel *T* than for steel *S*. The lines for second-order brown and blue also are lower for steel *T* than for steel *S*, except at the right end, where the corresponding lines in the two diagrams practically coincide.

The diagram for 25:20 chromium-nickel steel, *T* (fig. 14) is lower than the diagram for 24.4-percent-chromium steel, *P*, (fig. 10), except at the upper-right corner. At this corner, the diagram for the chromium-nickel steel is slightly higher than that for the chromium steel. The evidence presented in figure 14, therefore, appears to confirm the evidence in figure 13, that the presence of nickel did not increase resistance to oxidation, except for film thicknesses greater than those corresponding to first-order colors. The larger percentages of nickel and chromium in the 25:20 alloy, have not made the resistance to oxidation greater than that of the 18:8 alloy; the 25:20 alloy was actually somewhat inferior to the 18:8 alloy. Whether such relationship is typical for steels of these compositions, however, could be determined only by additional experiments with other samples.

In figure 15 is a diagram representing an alloy containing 13.4 percent of chromium and 78.6 percent of nickel. As the iron in this alloy amounted to only about 7 percent, the alloy cannot be classed as a steel. Alloys consisting chiefly of chromium and nickel, however, are much used in services requiring resistance to oxidation at elevated temperatures. It may be of interest, therefore, to compare alloy *U* with the high-chromium steels and chromium-nickel steels. Because of the scatter of experimental points in figure 15, the diagram is less exactly established than are most of the diagrams previously discussed; it may, however, be considered approximately correct.

The diagram for alloy *U* (fig. 15) differs little in form and position from the diagrams for the 24.4-percent-chromium steel, *P* (fig. 10),

and the 18:8 chromium-nickel steel, *S* (fig. 13). Line *U* in figure 16, representing first order-straw color, is somewhat higher than line *S*; it is also higher than line *P*, except at the left end. Lines *U* in figures 17 and 18, representing first-order brown and blue, are considerably lower than lines *S* and *P*. Line *U* in figure 19, representing second-order blue, is higher than line *S*, and much higher than line *P*. Although the evidence is not entirely consistent, it appears to confirm the evidence obtained with chromium-nickel steel, *S*, that nickel in conjunction with high percentages of chromium tends to increase the resistance to oxidation after the film has grown to thicknesses corresponding to second-order colors. This subject, however, needs further investigation.

6. AN EQUATION TO REPRESENT THE INFLUENCE OF TEMPERATURE ON OXIDATION TIME, FOR CONSTANT FILM THICKNESS

The linear relationship represented by the corrected graphs in figures 1 to 15, inclusive, means that the oxidation time varies inversely, and that the mean rate of oxidation varies directly, as a power of the absolute temperature. This relationship may be represented by the equation:

$$\log t_2 - \log t_1 = n (\log T_1 - \log T_2). \quad (7)$$

In this equation, $\log t_1$, $\log T_1$, $\log T_2$, and $\log T_2$ represent the coordinates of two points on a straight-line graph, and n represents the cotangent of the angle of slope, when the coordinates represent the first power of each variable. Because the tenth powers of the absolute temperatures are used as ordinates in figures 1 to 15, the cotangents of the angles of slope in these figures must be multiplied by 10 to obtain the corresponding values of n .

Equation 7 may be changed to the form

$$t_2/t_1 = (T_1/T_2)^n, \quad (8)$$

which shows that the oxidation time (for constant film thickness) varies inversely as n th power of the absolute temperature. The mean rate of oxidation, because it is proportional to the reciprocal of the oxidation time, varies directly as the n th power of the absolute temperature.

Values for " n " obtained from the slopes of the graphs of figures 1 to 15, have been assembled in table 2. For each alloy represented in the table, " n " increases with the progression of interference colors from first-order straw color to the last discernible color. The range of values of " n " varies with the amount of divergence of the lines in the corresponding diagram. The 0.46- and 0.83-percent carbon steels, *D* and *E*, whose diagrams are higher than those of steels with smaller or larger percentages of carbon, gave much wider ranges of " n " than those of the other steels. The average values for the carbon steels, with the exception of steels *D* and *E*, differ little from the corresponding averages for alloy tool steels, low-chromium steels, and stainless chromium-nickel alloys, *S*, *T*, and *U*. They also differ little from the values for chromium-silicon steel, *Q*, and from all the values for the 24.4-percent-chromium steel, *P*, except the low value for first-order straw color.

Considerably greater ranges of values, comparable with the ranges for steels *D* and *E*, were obtained with nickel steels, *J* and *K*. A smaller range of values was obtained with 13.6-percent-chromium steel, *O*. As previously stated, however, the diagram for this steel is less exactly established than the diagrams for most of the other steels. Low values for "*n*" were also obtained with the complex alloy, *R*. With the exceptions that have been mentioned, the steels show little difference in corresponding values for "*n*." The significance of the exceptions could be determined only by experiments with samples from other heats of these compositions.

Pilling and Bedworth [22], as stated in section II (2), obtained a linear logarithmic relationship between the absolute temperature and an "oxidation rate constant" estimated on the assumption of a parabolic relationship between oxidation time and the thickness of the oxide layer. In their experiments, however, the oxide layers were 10 to 1,000 times as thick as films giving interference colors. The value of "*n*" for iron, obtained from their data, is 19.3, which is much smaller than the value (39.7) listed in table 2 for iron with film thickness corresponding to third-order blue. Because "*n*" increases with film thickness, for all the steels listed in table 2, a higher rather than a lower value would be expected for the relatively thick oxide layers obtained by Pilling and Bedworth [22]. Further discussion of the relationship between values obtained with thin films and with relatively thick layers is given in sections V and VI.

V. VARIATION OF FILM THICKNESS WITH TIME, AT CONSTANT TEMPERATURE

1. DERIVATION OF DIAGRAMS

Each diagram of figures 1 to 15 represents a plan view of a three-dimensional diagram, in which the vertical dimension represents film thickness. The graphs in each diagram of these figures, therefore, may be viewed as contour lines. The film thickness corresponding to a contour line, which represents a constant interference color, increases with the progression of interference colors from first-order straw color to third-order blue. A plan view, therefore, gives qualitative information about the form of the three-dimensional diagram. For more definite information, both qualitative and quantitative, it is necessary to consider not only the plan view, but also the front view and side elevation. The front view gives direct information about the variation of film thickness with time at constant temperature. Diagrams of front views, derived from typical diagrams of figures 1 to 15, are shown in figures 21 to 24 and figure 26, and typical curves taken from these diagrams are compared in figure 25.

For construction of diagrams of this type, it is necessary to have information about the relationship between film thickness and interference color. The relationship between film thickness (*y*), wave length (λ), index of refraction (μ), and the order (*b*) of the interference color, is expressed by the equation

$$2y = \frac{(2b-1)\lambda}{2\mu}. \quad (9)$$

According to this equation, the film thicknesses for the same color of the first three orders are in the ratio 1:3:5. This equation is based

on the assumption that a change of 180° in phase occurs in the light reflected from both the air-oxide interface and the oxide-metal interface. Some investigators, however, have concluded that the 180° change of phase occurs only in the light reflected from the outer surface of the oxide film. On this assumption, light interference would occur when the film thickness is an even multiple of half the wave length, and the ratio of film thicknesses for the same color of the first three orders would be 1:2:3. There is strong evidence, however, in favor of the assumption involved in eq 9. Evans [8] has reported that the color of an oxide film, stripped from the metal and viewed by reflected light, is complementary to the color observed when the film was on the metal. Such a relationship is in accordance with the assumption that light reflected from the oxide-metal interface undergoes a 180° change in phase. Evidence in favor of the 1:3:5 relationship between film thicknesses for the same color of the first three orders has been reported by Dunn [4] on the basis of measurement of electrical conductivity of oxide films. Similar evidence based on weight measurements was obtained by Constable [1], by Vernon [39], by Evans and Miley [9], and by Miley and Evans [20]. Estimated film thicknesses in figures 21 to 26, therefore, are based on the assumption involved in eq 9.

The absolute thickness of the oxide film cannot be determined accurately by means of interference colors, because of lack of exact information about the index of refraction. The index of refraction varies with the composition of the oxide film and with the wave length of the incident light.⁷ The influence of variations of composition on the index of refraction probably is slight for the oxide films on iron or steel. If the index of refraction did not vary with wave length, therefore, approximate relative values of film thickness could be obtained by using a constant value (such as 1.0) for " μ " in eq 9. The phenomena of dispersion of light, however, show that the index of refraction generally varies with the wave length. Even approximate relative values of film thickness, therefore, cannot be obtained without making allowance for the influence of wave length on the index of refraction.

Conclusive evidence is lacking as to the influence of wave length on the index of refraction of the oxide film on iron or steel. Results of investigation applicable to this problem were obtained by Constable [2], with oxide formed by ignition of iron in air. His results indicate that the index of refraction is about 15 percent greater for brown interference color, and 25 to 30 percent greater for straw color, than for blue. It is not certain, however, that these values represent the approximate variation of the index of refraction of the oxide film on iron or steel.

Extrapolation of values of the index of refraction of hematite, recorded in the International Critical Tables for a range of wave length from 5890 to 7600 Å (angstrom units), gives a much smaller variation with wave length, about 15 percent for the range from straw color to blue. To avoid overcorrection in estimating the relative values of film thickness for use in figures 21 to 26, therefore, it has been assumed that the variation of the index of refraction with variation of the interference color from straw color to blue is 15 percent.

⁷ In a recent circular referring to an investigation (not yet published) at Carnegie Institute of Technology, it is said that the index of refraction varies appreciably with the temperature. If so, the film thickness represented by a graph in figures 1 to 15 is not quite constant. The variation, however, probably is slight.

In estimating thicknesses for use in these diagrams, consequently, an uncorrected value for each interference color was obtained by using a value of 1.0 for μ in eq 9. To allow for the variation of μ with wavelength, different corrections were then applied for the different interference colors. No correction was applied to the values for blue, of the three orders, but deductions of 7½ percent and 15 percent were made from the uncorrected values for brown and straw color, respectively.

The wave length corresponding to each interference color used in calculations of film thickness was determined by spectrophotometric measurements. Eighteen specimens, six for each of the interference colors used, were submitted to the Optical Division of the Bureau for examination by means of a recording spectrophotometer. Six spectral reflectance curves were thus obtained for each of the three colors. The agreement in form and position of these six curves was so close that the relationship for each color has been represented by a single curve of mean values in figure 20. The results of these measurements thus indicate that the interference colors can be distinguished accurately by use of the unaided eye.

The wave lengths for minimum reflectance may be readily estimated from the curves (fig. 20) obtained with the blue and brown interference colors. Although no minimum appears in the curve for straw color, the curve apparently is approaching a minimum, which would be at a wave length somewhat below the limit of the recording spectrophotometer (4000 Å). A value of 3500 Å has been assumed for this minimum. For brown and blue, the corresponding values are 4410 and 6330 Å, respectively. By use of these values, corresponding values for film thickness have been calculated by means eq 9. These values, corrected as previously indicated, have been used in constructing the ordinate scales for figures 21 to 26.⁸

2. GENERAL DESCRIPTION OF DIAGRAMS

Abscissas in these front views of three-dimensional diagrams, like abscissas in the plan views (figs. 1 to 15), represent the logarithms of the first powers of the oxidation times. The scale of abscissas, however, is more condensed in the front views than in the plan views. The ordinates, for convenient representation of the slight slope of the curves at the left, represent the logarithms of the tenth powers of the thicknesses. The interference colors, from first-order straw color to third-order blue, are indicated at the right of each figure. The letters used to designate these colors have the significance indicated in the general legend, the same significance as in figures 1 to 15.

The diagrams of figures 21 to 24 are derived from typical diagrams of figures 1 to 15. Each small open circle in figures 21 to 24 corresponds to a point on one of the straight graphs of the plan view; each black circle corresponds to a point obtained by extrapolation of one of these straight graphs. Each curve of figures 21 to 24 is based not only on the corresponding small circles, but also on the interrelationship between all the curves of the diagram, and on the interrelationship between the front view, plan view, and side elevation (figs. 27 and 28, and section VI) of the three-dimensional diagram.

The eight diagrams in figures 21 to 24 are similar in form, but differ in position on the coordinate scales. Each curve represents the vari-

⁸ The same values have been used in constructing diagrams of a different type, figures 27 and 28.

ation of film thickness with time at the indicated constant temperature. All the curves are qualitatively similar, and are very different in form from the contour lines shown in the plan views.

3. FORM OF THE CURVES OF VARIATION OF FILM THICKNESS WITH TIME, AT CONSTANT TEMPERATURE

The slope of a logarithmic curve of variation of film thickness with oxidation time, is slight at the left, but increases gradually as the curve extends to the right. At the upper boundary of the diagram, each curve appears to be approaching a sloping asymptote. The slope of the logarithmic curve at any point may be represented by the equation

$$\frac{d \log y}{d \log t} = dy/dt \cdot t/y = m. \quad (10)$$

In this equation, y and t have the same significance as in previous equations, and m represents the tangent of the angle of slope at any point, when the coordinates represent the first powers of the two variables. When the tenth power of the thickness is plotted against the first power of the time, as in figures 22 to 24, m is one-tenth the tangent of the angle of slope.

At film thicknesses corresponding to third-order blue, the upper curves in each diagram are nearly straight, and evidently differ little in slope from the corresponding asymptotes. The slopes of the asymptotes of the uppermost curves (represented by a broken line), moreover, are about the same in each diagram. The tangent of the angle of this slope is about 5, thus indicating that m is about 0.5. For any except the upper curves in each diagram, the slopes of the asymptotes cannot be determined even approximately. Probably, however, the asymptotes of all the curves in all the diagrams have about the same slope, corresponding to a value of about 0.5 m . A straight line with this slope represents a quadratic parabola. As each curve extends to the left, m decreases, and eventually becomes very small, probably less than 0.01.

In the experiments on which figures 21 to 24 are based, the initial film thickness was not zero. As stated in section III, the specimens after polishing were kept in dry air at room temperature until needed for experiment. Under such conditions each specimen acquired an invisible oxide film. The few experiments made to determine the thickness of such invisible oxide films, have led to widely differing conclusions. Freundlich, Patscheke, and Zoehrer [11], who used polarimetric methods, reported that iron mirrors, prepared by thermal decomposition of iron carbonyl in a vacuum and then exposed to air for 10 seconds or less, acquired an oxide film about 10 Angstrom units thick. Tronstad and Höverstad [33], who also used polarization methods, reported that the oxide film on polished iron surfaces in air was about 20 Å thick. The accuracy obtainable by the polarization method, however, is somewhat doubtful. Much greater thickness of the oxide film formed at room temperature was reported by Miley [18]. The thickness of the film formed on iron, in 1 day in a desiccator at 18° C, was reported to be 230 Å. Assuming the index of refraction to be about 2, the equivalent air thickness (for comparison with the scale of thickness used in figs. 21 to 24) would be about 450 Å, which is more than half the estimated value for first-order straw color.

Even on the assumption that the relatively high value reported by Miley is correct, it can be shown that the correction to be applied to the observed oxidation time, to make allowance for the time required to form the initial film, is negligible. The amount of such correction is indicated by the equation

$$t_1/t = (y_1/y)^{1/m}. \quad (11)$$

In this equation, t represents the total correct time, t_1 represents the time necessary to form the initial film, y represents the final film thickness, and y_1 represents the initial thickness. Even assuming a value of 0.5 for y_1/y at first straw color, the corresponding value of $1/m$ is so large (10 or more) that the correction to be applied to the observed oxidation time would be only about 0.1 percent. Such correction would make no appreciable change in any of the curves of figures 21 to 24.

The increase in slope of each curve in figures 21 to 24, as it extends to the right, does not necessarily mean that the rate of oxidation (rate of increase of film thickness with time, dy/dt) increases with increase in film thickness. A curve with downward convexity when drawn with logarithmic coordinates, may become a curve with upward convexity when drawn with Cartesian coordinates, provided that m is less than 1.0, and that the curvature of the logarithmic graph is not too great. As m never exceeds 0.5, the former condition exists. That the latter condition exists can be determined only by plotting the curves with Cartesian coordinates. This has been done in the diagrams of figure 26.

Film thickness, in figure 26, is plotted against the square root of the oxidation time. This method of plotting was chosen to increase the practicable range of oxidation time that can be represented, and also because the asymptotic value of m for the logarithmic curves corresponds to a quadratic parabola. A straight line passing through the origin in a diagram such as those of figure 26, would represent a quadratic parabola, and thus would represent continuous decrease of oxidation rate with increase in film thickness. The upward convexity of the graphs, therefore, indicates that the decrease in velocity of oxidation with increase in film thickness is more rapid than that corresponding to a quadratic parabola. The strong initial curvature of these graphs, the gradual decrease in curvature, and the approach to approximate straightness, are in accordance with the corresponding variation of m (figs. 21 to 24) from less than 0.01 to about 0.5. The initial rate of oxidation, as shown in figure 26, is so great that the first part of each curve appears vertical, up to a film thickness (air equivalent) of about 600 Å. At and near the origin, the slope of each curve is governed largely by the rate of chemical combination of iron and oxygen (in absence of an impeding film). With the formation and increase in thickness of the film, the rate of oxidation decreases. At first this decrease in velocity is extremely rapid, in accordance with a parabola of high degree. The rate of decrease of velocity, however, rapidly decreases, and eventually reaches a value represented approximately by a quadratic parabola, which would correspond to an approximately linear relationship in figure 26. (The approach to a quadratic parabola is indicated only qualitatively by the approach to straightness of the graphs in fig. 26, because the approximately quad-

ratio portion of each curve does not pass through the origin of coordinates.)

As shown in section II (1), Pilling and Bedworth [22] and others have reported that the relationship between oxidation time and the thickness of the oxide layer is represented by a quadratic parabola, eq. 2. Their results, however, are based on experiments with oxide layers 10 to 1,000 times as thick as films corresponding to interference colors. As shown by the curves in figures 21 to 24 and figure 26, a quadratic parabola is not a generally correct representation of the variation of film thickness with time at constant temperature. The curves, however, do indicate approach to a quadratic relationship with increase in film thickness. At rapid rates of oxidation, the quadratic relationship is approached closely when the film thickness reaches a value corresponding to third-order blue. At slow rates of oxidation, this relationship is not nearly approached until the thickness of the oxide layer is much greater.

The range of oxygen concentration from the outer to the inner surface of the film, according to implication of the theory of Pilling and Bedworth [22], does not vary with film thickness. The curves in figures 21 to 24 and in figure 26, however, indicate that either the range of oxygen concentration or the diffusional conductivity is (or both are) greater for thin films than for relatively thick films. The thinnest possible film may have at first a layer of 100-percent oxygen adjacent to a layer of 100-percent iron; this would be the greatest possible range of oxygen concentration. With diffusion and with increase in film thickness, the range of concentration would decrease rapidly. Whether such variation in the oxygen concentration-range with film thickness would account for the course of curves such as those in figures 21 to 24, however, cannot be determined without additional evidence. The diffusional conductivity, as well as the concentration range, possibly decreases with the growth of the film throughout the range of interference colors.

4. COMPARISON OF TYPICAL DIAGRAMS

The ranges of coordinates are the same in all the diagrams of figures 21 to 24. The relative resistance to oxidation of the typical metals represented by these diagrams, therefore, may be studied by comparing the indicated ranges of temperature. In the diagrams for electrolytic iron, *A*, and 0.85-percent-carbon steel, *E* (fig. 21), and in the diagram for 5-percent-chromium steel, *N* (fig. 22), the temperatures represented by the highest and lowest curves are 350° and 100° C, respectively. In the diagrams for the 13.6-percent-chromium steel, *O* (fig. 22), for steel *Q* containing 8.8 percent of chromium and 2.8 percent of silicon (fig. 23), and for the stainless chromium-nickel alloys, *S*, *T*, and *U* (figs. 23 and 24), the temperatures represented by the highest and lowest curves are 900° and 300° C, respectively. In the diagram for 24.4-percent-chromium steel, *P* (fig. 23), the temperature range is from 900° to 400° C.

For closer comparison, typical curves from the diagrams of figures 21 to 24, and a curve for a steel (*R*) not represented in these figures, are assembled in figure 25. Considerable extrapolation was required in extending the diagram over this wide range of abscissas. At 300° C, comparison is made between electrolytic iron, *A*; 0.83-percent-carbon steel, *E*; 5-percent-chromium steel, *N*; and 13.6-percent-chromium

steel, *O*. A 400° C curve is used for steel *R*, because a 300° C curve would conflict with the group of curves representing 500° C. At 500° C, comparison is made between five steels with relatively high resistance to oxidation. A curve for the chromium-nickel-iron alloy, *U*, is not included in this group because it would follow closely the curve for chromium-nickel steel, *T*.

Curves *A* and *E*, representing electrolytic iron and 0.83-percent-carbon steel at 300° C, differ little in form and position. The relative positions, however, indicate that steel *E* is slightly superior in resistance to oxidation, especially at thicknesses greater than those corresponding to first-order colors. The relative positions of these two curves are in accordance with the relative positions of the corresponding graphs in the plan views, figures 16 to 19. The curve for 5-percent-chromium steel, *N*, diverges from curves *A* and *E* at a thickness corresponding to first-order straw color, and extends to the right of these curves, thus indicating increasing superiority for steel *N* with increase in film thickness. The relative positions of curves *R* and *N* indicate that a curve representing steel *R* at 300° C, instead of 400° C, would extend to the right of curve *N*. The superiority of steel *R*, thus indicated, probably is due chiefly to its larger percentage of chromium.

The curve representing 13.6-percent-chromium steel, *O*, at 300° C, if extended far enough to the left, probably would cross the curves representing electrolytic iron, carbon steel, and 5-percent chromium steel. To the left of the intersection, according to this evidence, carbon steel and 5-percent-chromium steel would be superior to the 13.6-percent-chromium steel. To the right of the intersection, the 13.6-percent-chromium steel is superior, and the superiority increases rapidly with increase in film thickness. The duration of heating required to reach first-order blue would be more than 10^7 times as great for the 13.6-percent-chromium steel as for carbon steels.

The curves of the group representing steels at 500° C differ little in position at very small film thicknesses. With increase in film thickness, the curves first diverge, then converge, and some of the curves intersect. Although the curves representing 13.6-percent-chromium steel, *O*, and 24.4-percent-chromium steel, *P*, intersect at about second-order straw color, they differ little in position to the right of the intersection. The accuracy of determination of the relative positions of these curves, however, is not great enough to justify the assumption that a steel containing 13.6 percent of chromium actually becomes superior to a steel containing 24.4 percent of chromium, when the film thickness exceeds a value corresponding to first-order blue. The evidence should rather be interpreted to mean that, at these film thicknesses, the two steels show practically no difference in resistance to oxidation. Throughout the range of film thickness corresponding to first-order colors, however, the 24.4-percent-chromium steel was found definitely superior to the 13.6-percent-chromium steel.

Curve *Q*, representing the steel containing 8.8 percent of chromium and 2.8 percent of silicon, coincides with curve *O* at interference colors beyond second-order brown. As they extend to the left, however, the two curves diverge. Throughout the range of first-order colors, curve *Q* is between curves *O* and *P*. Throughout this range of colors, therefore, the steel containing 8.8 percent of chromium and 2.8 percent of silicon was superior to the 13.6-percent-chromium steel, but inferior

to the 24.4-percent-chromium steel. With further extension to the left, the three curves again converge.

The curve for 18:8 chromium-nickel steel, *S*, differs little in position from the curve for 24.4-percent-chromium steel, *P*, until the film thickness exceeds a value corresponding to first-order brown. With further increase in film thickness, curve *S* extends to the right of curve *P*, thus indicating superiority of the chromium-nickel steel throughout a range of thicknesses corresponding to second- and third-order colors. The curve for 25:20 chromium-nickel steel, *T*, is above curves *P* and *S* throughout the range of first-order colors and part of the range of second-order colors. With further increase in film thickness, however, curve *T* extends to the right of curves *P* and *S*. A curve for chromium-nickel-iron alloy, *U*, if drawn in this diagram, would practically coincide with curve *T*.

The evidence obtained with the three chromium-nickel alloys, *S*, *T*, and *U*, therefore, indicates some superiority of these alloys over high-chromium steels for film thicknesses corresponding to second- and third-order colors, and possibly superior resistance to scaling at still greater thickness of the layer of oxide. For film thicknesses corresponding to first-order colors, the chromium-nickel alloys showed some superiority over the 13.6-percent-chromium steel, but no superiority over the 24.4-percent chromium steel.

At the left ends, the curves representing 500° C are much less steep than the curves representing electrolytic iron, carbon steel, and 5-percent-chromium steel at 300° C. This difference in slope would be even greater, if comparison were made at the same temperature; the curves representing carbon steels and 5-percent-chromium steel probably would cross all the curves representing the corrosion-resisting steels. (The evidence for this relationship is more clearly revealed in figs. 27 and 28, by comparison of entire diagrams of a different type, described in section VI.) For very thin films, therefore, resistance to oxidation at elevated temperatures evidently is less for corrosion-resisting steels than for carbon steels or for steels containing 5 percent (or less) of chromium.

Additional evidence that chromium and some other alloying elements first increase and then decrease the rate of oxidation, is given by Portevin, Prétet, and Jolivet [23, 24]. This effect is exhibited by elements, such as silicon, aluminum, and chromium, whose affinity for oxygen is greater than that of iron (as shown by the greater heats of formation of their oxides). These investigators reported that, because chromium tends to oxidize more rapidly than iron, the oxide of chromium eventually becomes concentrated in a thin layer at the inner surface of the oxide film. Through this layer, diffusion is less rapid than through oxide of iron. Until enough chromium has been oxidized to build up this thin layer of oxide of chromium with a superimposed layer consisting chiefly of oxide of iron, the rate of oxidation of chromium steel is greater than that of carbon steel. With increase in film thickness beyond this point, the rate of oxidation is less for chromium steel than for carbon steel. If the percentage of chromium in the steel is 13 percent or more, the protective effect of the chromium begins when the film is very thin.

VI. VARIATION OF FILM THICKNESS WITH TEMPERATURE, FOR CONSTANT OXIDATION TIME

1. GENERAL DESCRIPTION OF DIAGRAMS

Most of the reported results of investigation of oxidation of metals at elevated temperatures represent determinations of increase of weight during a fixed time at various temperatures. These results, therefore, give direct information about the variation of thickness of the oxide layer with temperature, for constant oxidation time. Diagrams representing the results, consequently, would be side elevations of three-dimensional diagrams, of the type that has been studied in plan and front views in sections IV and V. As the results were obtained with rapid rates of oxidation and with relatively thick oxide layers, however, they give no information as to the course of the curves throughout the side elevation, especially at film thicknesses corresponding to interference colors. To obtain information about the form of such curves, and to obtain complementary information about the forms of the three-dimensional diagrams, therefore, left-side elevations of typical diagrams have been assembled in figures 27 and 28.

The logarithmic coordinates in these diagrams represent the tenth powers of temperature and film thickness. The scale dimension, however, is twice as large for abscissas as for ordinates. The tenth power of each variable is used in these side elevations because the tenth powers of the same variables are used in the plan views and front views. A curve in such a diagram, however, is identical in form with the corresponding curve in a diagram with coordinates representing the first power of each variable. For correct representation of the left-side elevations, abscissas in figures 27 and 28 read from right to left.

The side elevation can be derived from either the plan view or the front view. The small circles and triangles in figures 27 and 28 were derived from corresponding points on graphs of the plan views. Each curve is based not only on the positions of the corresponding symbols, but also on the probable interrelationship between all the curves of the diagram, and on the proper interrelationship between the side elevation and the corresponding plan and front views.

2. FORM OF THE CURVES OF VARIATION OF FILM THICKNESS WITH TEMPERATURE, FOR CONSTANT OXIDATION TIME

The logarithmic curves in the side elevations (figs. 27 and 28) are qualitatively similar to the logarithmic curves in the front views (figs. 21 to 24). The slope increases with temperature and with film thickness. With approach to the upper boundary of the diagram, the curvature decreases continuously, and each curve apparently approaches a steeply sloping asymptote. The slope of a curve at any point is represented by the equation

$$\frac{d \log y}{d \log T} = dy/dT \cdot T/y = h \quad (12)$$

In this equation, y and T have the same significance as in previous equations, and h represents the tangent of the angle of slope at any point. Because of the difference in dimensions of the abscissa and ordinate scales in figures 27 and 28, h is one-half the tangent of the angle of slope of a curve (at any point).

From the range of values of h , represented by each logarithmic curve, may be deduced the probable form of a corresponding curve drawn with Cartesian coordinates. The extreme range of values of h for all the curves in figures 27 and 28, is between about 0.2 and 25. Throughout most of the represented extent of each curve (throughout the entire represented extent of some curves), however, h is greater than 1.0. Curves drawn with Cartesian coordinates, therefore, evidently should be qualitatively similar, except possibly in their lower portions, to the curves in figures 27 and 28. Curves actually plotted with Cartesian coordinates, but not here shown, give no evidence of reversal in the lower portions; the slope increases continuously with increase in temperature (and with increase in film thickness). The accelerating influence of rise of temperature, on the rate of oxidation, thus predominates over the retarding influence of increase of film thickness (for constant oxidation time).

The curves in the side elevation of a three-dimensional diagram, if drawn with Cartesian coordinates, are dissimilar in form to the curves so drawn in the front elevation (fig. 26). A three-dimensional diagram, when plotted with Cartesian coordinates, therefore, is complex in form; the graphs in the plan view as well as in the front view are strongly curved. This type of diagram will not be considered in detail.

The asymptotes of the curves in all the diagrams of Figures 27 and 28 apparently differ little in slope. The approximate slopes of these asymptotes may be deduced from the slopes of curves at corresponding points in the plan view and front view. The relationship between the tangent (h) of the angle of slope in the side elevation, the tangent (m) of the angle of slope in the front view, and the cotangent (n) of the angle of slope of the plan view, is given by the equation:

$$h = mn \quad (13)$$

By means of this equation and by use of the asymptotic values for m and n given in section V (3) and in table 2, corresponding values of h may be estimated. The tangent (m) of the angle of slope of the asymptote approached by each curve in a front elevation, as shown in section V (3) probably is about 0.5. The values of n corresponding to second-order blue, for steels A , E , O , and P (represented in figs. 27 and 28) are 38.5, 51.0, 32.8, and 35.7, respectively. By substituting these values for m and n in eq 13, the corresponding values obtained for h are 19, 25, 16.5, and 18. With allowance for the 2:1 ratio of scale dimensions in figures 27 and 28, corresponding tangents of the angles of slope of the asymptotes in these figures should be 9.5, 13, 8, and 9. These values are approximately in accordance with the slopes of the curves at the upper boundaries of the diagrams.

As shown in section II (3), results obtained by Dickenson [3] with steels at various temperatures, with constant oxidation time, led him to conclude that logarithmic plotting gives a linear relationship between temperature and the thickness of the oxide layer. Much thicker oxide layers, however, were obtained in his experiments than in experiments based on observation of interference colors. No graphs with logarithmic coordinates were published by Dickenson, and no values were given for the tangent of the angle of slope. From some of his published data, however, it is possible to plot such graphs. Although the graphs so plotted show wide scatter of experimental values, they conform approximately to a linear logarithmic relation-

ship. Values of h so obtained, for the six steels investigated by Dickenson, range from about 11 to 18. These values are generally smaller than the values (16.5 to 25) obtained from the upper ends of the curves in figures 27 and 28. As shown in these diagrams, moreover, the relationship between temperature and film thickness, for constant oxidation time, cannot be represented by any single equation. For constant oxidation time, the film thickness increases as an increasing power of the absolute temperature. With increase in film thickness, the exponent of the power increases from 1 or less to about 20 or 25.

As the logarithmic curves in the front and side elevations of a three-dimensional diagram apparently approach sloping asymptotes, the surface of the three-dimensional diagram (with increase in film thickness) probably approaches a steeply sloping asymptotic plane.

3. COMPARISON OF TYPICAL DIAGRAMS, REPRESENTING THE VARIATION OF FILM THICKNESS WITH TEMPERATURE

In each of figures 27 and 28 are two diagrams representing steels differing greatly in resistance to oxidation. One of the diagrams in each figure represents a carbon steel or iron, the other represents a high-chromium steel. Figure 28 contains also a diagram representing a steel with intermediate resistance to oxidation, a 5-percent-chromium steel. The range of oxidation time is the same in each diagram.

For film thicknesses beyond a value represented by a color between first-order straw color and brown, the temperature field traversed by the diagram representing the high-chromium steel (in each figure) is higher than that traversed by the diagram representing the carbon steel or iron. In the lower part of each figure, however, the diagram representing the high-chromium steel crosses the diagram representing the carbon steel or iron. The diagram representing the 5-percent-chromium steel (fig. 28) crosses both the diagram representing the carbon steel and the diagram representing the 24.4-percent-chromium steel. With increase in film thickness, the curves for the 5-percent-chromium steel extend to the left of the corresponding curves representing the carbon steel, but to the right of the curves representing the high-chromium steel.

The relative resistances to oxidation of these typical steels, revealed by comparison of side elevations of entire three-dimensional diagrams, are in accordance with those revealed by comparison of single curves in the front view, figure 25. The diagrams in figures 27 and 28 confirm the evidence in figure 25, that the resistance to oxidation of chromium steels is less than that of carbon steels until the film thickness exceeds a value corresponding to one of the interference colors of the first order. Probable reasons for this relationship have been given in section V (4).

VII. SUMMARY

By use of interference colors, an investigation has been made of the variation of the thickness of the oxide film on steels, with temperature and time. The relationship between temperature, time, and film thickness, for each of various steels, has been represented by three views of a three-dimensional diagram. From such diagrams, information may be obtained about the influence of temperature and film thickness on the rate of oxidation. The relation between temperature

and time (for constant film thickness), when plotted with logarithmic coordinates, is linear. The slope of the graph indicates that the mean rate of oxidation varies directly, and the oxidation time varies inversely, as a high power (23 to 60) of the absolute temperature.

The variation of film thickness with time at constant temperature, when plotted with logarithmic coordinates, gives a curved line. The slope of this line increases with film thickness, and the line approaches a sloping asymptote; the tangent of the angle of slope of the asymptote is about 0.5. If over short intervals the oxidation time is assumed to vary as a power of the film thickness, the exponent decreases from a high value (100 or more) for thin films, to about 2 for relatively thick films. When plotted with Cartesian coordinates, the form of the curve indicates that the instantaneous rate of oxidation decreases continuously with increase in film thickness.

For constant oxidation time, the relation between film thickness and absolute temperature, when plotted with logarithmic coordinates, also gives a curved line. If for short intervals the film thickness is assumed to vary as a power of the absolute temperature, the exponent increases from 1 or less for thin films to about 20 or 25 for relatively thick films. The accelerating influence of temperature on the rate of oxidation (for constant oxidation time) thus predominates over the retarding effect of increasing film thickness.

By means of views of the three-dimensional diagrams, comparison is made between steels of various compositions, and the influence of alloying elements is discussed.

A tentative discussion is given of the relationship between the rate of oxidation and the constitution and physical properties of the oxide film. The rate of oxidation depends on the oxygen concentration gradient in the film, and on the diffusional conductivity of the oxide. Consideration is given to the possible relationship between these two factors and various physical properties, and to the influence of film thickness on this relationship.

VIII. REFERENCES

- [1] F. H. Constable, *Colors shown during oxidation of metallic copper*. Proc. Roy. Soc. (London) [A] **115**, 579 (1927).
- [2] F. H. Constable, *Spectrophotometric observations on the growth of oxide films on iron, nickel, and copper*. Proc. Roy. Soc. (London) [A] **117**, 376 (1928).
- [3] F. H. S. Dickenson, *Some experiments on the flow of steels at a low red heat, with a note on the scaling of heated steels*. J. Iron Steel Inst. **106**, 128 (1922).
- [4] J. S. Dunn, *The low temperature oxidation of copper*. Proc. Roy. Soc. (London) [A] **111**, 210 (1926).
- [5] J. S. Dunn, *High temperature oxidation of metals*. Proc. Roy. Soc. (London) [A] **111**, 203 (1926).
- [6] U. R. Evans, Discussion of paper "Oxidation of metals at high temperature"—N. B. Pilling and R. E. Bedworth, J. Inst. Metals **29**, 585 (1923).
- [7] U. R. Evans, *The colors due to thin films on metals*. Proc. Roy. Soc. (London) [A] **107**, 228 (1925).
- [8] U. R. Evans, *Metallic Corrosion, Passivity and Protection* (Edward Arnold & Co. London, 1937).
- [9] U. R. Evans and H. A. Miley, *Measurement of oxide films on copper and iron*. Nature **139**, 283 (1937).
- [10] W. Feitknecht, *Über die Oxydation des Kupfers bei hohen Temperatur*. Z. Elektrochem. **35**, 142 (1929).
- [11] H. Freundlich, G. Patscheke, and H. Zocher, *Über die Passivität von Eisen-spiegeln*. Z. physik. Chem. **130**, 289 (1927).
- [12] K. Heindlhofer and B. M. Larsen, *Rates of scale formation on iron and a few of its alloys*. Trans. Am. Soc. Steel Treating **21**, 865 (1933).

- [13] J. C. Hudson and T. E. Rooney, Review of Oxidation and Scaling of Heated Solid Metals, Sec. 3. (His Majesty's Stationary Office, London, 1935).
- [14] O. F. Hudson, T. M. Herbert, F. E. Ball, and E. H. Bucknall, *Properties of locomotive firebox stays and plates.—oxidation of arsenical copper and the effects of small quantities of added elements on the softening temperature and mechanical properties of copper.* J. Inst. Metals (London) **42**, 243 (1929).
- [15] A. F. Joffé, *The Physics of Crystals.* (McGraw-Hill Book Co. Inc., New York, N. Y., 1928).
- [16] A. Krupkowski and J. Jaszczurowski, *Vitesse d'oxydation des métaux à température élevée.* Congrès Int. Mines Métallurgie Géologie (Metallurgy) Paris, **2**, 329 (1935).
- [17] R. F. Mehl and E. L. McCandless, *Oxide films on iron.* Metals Tech. **4**, Tech. Pap. 780 (1937).
- [18] H. A. Miley, *The thickness of oxide films on iron.* Carnegie Scholarship Memoirs, Iron and Steel Inst. **25**, 197 (1936).
- [19] H. A. Miley and U. R. Evans, Summary of Work at Cambridge on the Electrometric Study of the Growth of Oxide Films. Fifth Rep. Corrosion Comm. Iron and Steel Inst., Spec. Rep. No. 21, Sec. D 243 (1938).
- [20] H. A. Miley and U. R. Evans, *The passivity of metals*, pt. 8. J. Chem. Soc. **1937**, 263.
- [21] D. W. Murphy, W. P. Wood, and W. E. Jominy, *Scaling of steel at elevated temperatures by reaction with gases and the properties of the resulting oxides.* Trans. Am. Soc. Steel Treating **19**, 193 (1932).
- [22] N. B. Pilling and R. E. Bedworth, *Oxidation of metals at high temperature.* J. Inst. Metals (London) **29**, 529 (1923).
- [23] A. M. Portevin, E. Prétet, and H. Jolivet, *Contribution to the study of the chemical resistance of various special steels.* J. Iron Steel Inst. (London) **130**, 219 (1934).
- [24] A. M. Portevin, E. Prétet, and H. Jolivet, *Méthodes d'étude de la corrosion des métaux et alliages par les gaz à température élevée et leurs applications.* Rev. met. **31**, 219 (1934).
- [25] L. E. Price, *Recent German advances in the mechanism of oxidation and tarnishing of metals.* Chemistry & Industry **15**, 769 (1937).
- [26] R. L. Rickett and W. P. Wood, *Action of oxygen and hydrogen sulphide upon iron-chromium alloys at high temperatures.* Trans. Am. Soc. Metals **22**, 347 (1934).
- [27] E. Schröder and G. Tammann, *Die Geschwindigkeit der Einwirkung von Sauerstoff, Stickoxyd und Stickoxydul auf Metalle.* Z. anorg. Chem. **123**, 179 (1923).
- [28] H. Schwarze, *Beitrag zur Kenntnis der Schutzwirkung der beim Zundern auf Stahl gebildeten Oxydschichten.* Mitt. Forsch.-Inst. Ver. Stahlwerke A-G. Dortmund, **2**, 263 (1932).
- [29] C. A. Siebert and C. Upthegrove, *Oxidation of a low carbon steel in the temperature range 1650 to 2100 degrees Fahrenheit.* Trans. Am. Soc. Metals **23**, 187 (1935).
- [30] G. Tammann and K. Bochow, *Vergleich der Oxydschichtdicke, bestimmt durch Anlauffarben und durch Wägung.* Z. anorg. Chem. **169**, 42 (1928).
- [31] G. Tammann and W. Koster, *Die Geschwindigkeit der Einwirkung von Sauerstoff, Schwefelwasserstoff und Halogenen auf Metalle.* Z. anorg. Chem. **123**, 216 (1922).
- [32] G. Tammann and G. Siebel, *Die Anlauffarben auf Eisen-Kohlenstofflegierungen und auf der Eisenmischkristallen.* Z. anorg. Chem. **143**, 297 (1925).
- [33] L. Tronstad and J. Höverstad, *Optische Untersuchungen zur Frage der Passivität der Metalle.* Z. physik. Chem. [A] **170**, 172 (1934).
- [34] C. Upthegrove, *Scaling of Steel at Heat-Treating Temperatures.* Eng. Res. Bul. Univ. Mich. No. 25 (1933).
- [35] C. Upthegrove and D. W. Murphy, *Scaling of steel.* Trans. Am. Soc. Steel Treating **21**, 73 (1933).
- [36] G. Valenski, *Introduction à la cinétique de l'oxydation des métaux donnant deux oxydes.* Compt. rend. **203**, 1252 (1936).
- [37] W. H. J. Vernon, *First report to Atmospheric Corrosion Research Committee.* Trans. Faraday Soc. **19**, 839 (1923).
- [38] W. H. J. Vernon, *Formation of protective oxide films on copper and brass by air exposure at various temperatures.* J. Chem. Soc. 2273 (1926).
- [39] W. H. J. Vernon, *Laboratory study of atmospheric corrosion of metals, pt. 2.—Iron: Primary oxide film.* Trans. Faraday Soc. **31**, 1668 (1935).
- [40] C. Wagner, *Beitrag zur Theorie des Anlaufvorganges.* Z. physik. Chem. [B] **21**, 25 (1933).

- [41] C. Wagner and K. Grünwald, *Beitrag zur Theorie des Anlaufvorganges III*. Z. physik. Chem. [B] **40**, 455 (1938).
 [42] F. J. Wilkins, *Über die Oxidation des Kupfers bei hohen Temperatur*. Z. Elektrochem. **35**, 500 (1929).

TABLE 1.—Chemical composition of steels

Symbol	Material ¹	Element, percentage by weight							Miscellaneous
		C	Mn	P	S	Si	Cr	Ni	
A	Electrolytic iron ²	0.008	0.003	-----	-----	0.001	-----	0.018	0.030 Cu.; 0.006 Co. 0.50 W. 2.74 W. 18.25 W; 1.12 V.
B	Open-hearth iron ²	.02	.03	-----	-----	.001	-----	-----	
C	0.09% C steel ²	.09	.56	-----	-----	.01	-----	-----	
D	0.46% C steel	.46	.57	0.036	0.042	.20	-----	-----	
E	0.83% C steel	.83	.27	.017	.015	.16	-----	-----	
F	1.29% C steel	1.29	.23	.017	.017	.23	0.05	-----	
G	Cr-W-Mn tool steel ²	1.00	1.20	-----	-----	-----	.50	-----	
H	2.74% W tool steel ²	1.34	0.25	.034	.054	.32	.14	-----	
I	High-speed steel	0.66	.26	.027	.012	.09	3.90	-----	
J	3.35% Ni steel	.40	.67	.034	.039	.23	-----	3.35	
K	31.95% Ni steel	.07	.81	-----	-----	.14	0.04	31.95	
L	1.38% Cr steel	1.06	.34	.016	.011	.19	1.38	-----	
M	2.18% Cr steel	0.72	.49	.025	.008	.19	2.18	-----	
N	5% Cr steel	{ .10 to 0.15	.50 max	{ .03	.03	.50	{ 4.0 to 6.0	-----	
O	13.6% Cr steel	.11	.55	.09	.066	.34	13.59	-----	
P	24.4% Cr steel	.15	.42	.013	.030	.23	24.4	0.35	
Q	8.8:2.8 Cr-Si steel	.45	.26	.012	.006	2.80	8.75	.21	
R	8.8:46.8 Cr-Ni steel	.20	.02	.01	.04	1.53	8.85	46.8	
S	18.2:8.6 Cr-Ni steel	.07	.44	.012	.018	0.50	18.22	8.63	
T	25:20 Cr-Ni steel	{ .25 max	.07	-----	-----	{ .7 to 1.5	24. to 26.	19. to 21.	
U	Cr-Ni-Fe alloy	.06	.53	-----	-----	-----	13.4	78.6	

¹ Iron is the remainder constituent in each of these steels.² Analysis by National Bureau of Standards; results not so designated are from mill analyses.TABLE 2.—Values for constant *n*, representing the variation of oxidation time with temperature, for constant film thickness

Symbol	Material	First-order			Second-order			Third-order blue
		Straw	Brown	Blue	Straw	Brown	Blue	
A	Electrolytic iron	30.0	30.4	31.1	33.6	36.0	38.5	39.7
B	Open-hearth iron	30.5	31.2	31.7	33.6	35.6	38.5	-----
C	0.09% C steel	31.7	34.3	35.8	36.1	37.0	38.0	-----
D	0.46% C steel	32.4	38.0	45.1	52.4	57.3	60.0	-----
E	0.83% C steel	30.3	35.6	42.7	44.7	48.4	51.0	-----
F	1.29% C steel	31.7	32.1	33.3	34.6	35.8	37.4	-----
G	Cr-W-Mn tool steel	31.7	32.1	32.9	33.1	33.2	33.3	-----
H	2.74% W tool steel	34.2	34.3	35.1	34.9	36.4	38.6	-----
I	High-speed steel	25.6	31.4	31.7	33.1	33.3	33.6	-----
J	3.35% Ni steel	31.5	35.9	43.2	45.1	46.6	47.3	-----
K	31.95% Ni steel	31.7	37.3	38.5	42.1	47.5	55.8	-----
L	1.38% Cr steel	28.8	31.6	34.1	35.8	38.1	41.0	-----
M	2.18% Cr steel	28.9	33.2	34.5	35.3	36.0	36.2	-----
N	5% Cr steel	25.5	29.7	36.4	-----	-----	-----	-----
O	13.6% Cr steel	31.7	32.1	32.3	32.6	33.0	32.8	-----
P	24.4% Cr steel	23.0	33.1	34.3	34.7	35.5	35.7	36.1
Q	8.8% Cr, 2.8% Si steel	25.8	28.6	30.9	31.5	31.9	32.3	-----
R	8.8% Cr, 46.8% Ni steel	23.7	23.7	24.3	-----	-----	-----	-----
S	18.2% Cr, 8.6% Ni steel	28.8	30.5	31.5	32.1	33.3	35.1	-----
T	25% Cr, 20% Ni steel	29.7	32.6	34.6	37.3	38.4	46.8	49.6
U	Cr-Ni-Fe alloy	30.8	31.9	33.7	34.0	33.9	33.9	-----

AVERAGE VALUES

A, B	Irons	30.2	30.8	31.4	33.6	35.8	38.5	-----
C, D, E, F	Carbon steels	31.1	33.6	36.6	39.2	41.7	43.9	-----
G, H, I	Alloy tool steels	30.5	32.6	33.2	33.7	34.3	35.2	-----
L, M	Low-Cr steels	28.9	32.4	34.3	35.5	37.1	38.6	-----
S, T, U	Cr-Ni stainless alloys	29.8	31.7	33.3	34.5	35.2	38.6	-----

GENERAL LEGEND

INTERFERENCE COLOR	DESIGNATION	FILM THICKNESS, ANGSTROM UNITS	EXPERIMENTAL POINTS, FIGURES 1—15	
FIRST ORDER STRAW	X	745	○	△ *
FIRST ORDER BROWN	Y	1025	∅	△
FIRST ORDER BLUE	Z	1580	●	▲
SECOND ORDER STRAW	X ₂	2235	□	
SECOND ORDER BROWN	Y ₂	3075	⊠	
SECOND ORDER BLUE	Z ₂	4740	■	
THIRD ORDER BLUE	Z ₃	7900	◆	

* TWO DIFFERENT SYMBOLS ARE USED WHEN TWO DIAGRAMS ARE SHOWN IN THE SAME FIGURE.

AN ARROW ATTACHED TO A SYMBOL INDICATES BY ITS DIRECTION THAT CORRECT TIME IS GREATER OR LESS THAN REPRESENTED.

NUMERALS ADJACENT TO A SYMBOL INDICATE THE NUMBER OF EXPERIMENTAL VALUES REPRESENTED BY THAT SYMBOL.

THICKNESS IS REPRESENTED IN CORRECTED AIR-EQUIVALENT VALUES.

IN FIGURES 21 TO 24, THE OPEN CIRCLES REPRESENT VALUES OBTAINED DIRECTLY FROM TEMPERATURE-TIME GRAPHS. THE CLOSED CIRCLES REPRESENT VALUES OBTAINED FROM EXTRAPOLATION OF THE TEMPERATURE-TIME GRAPHS.

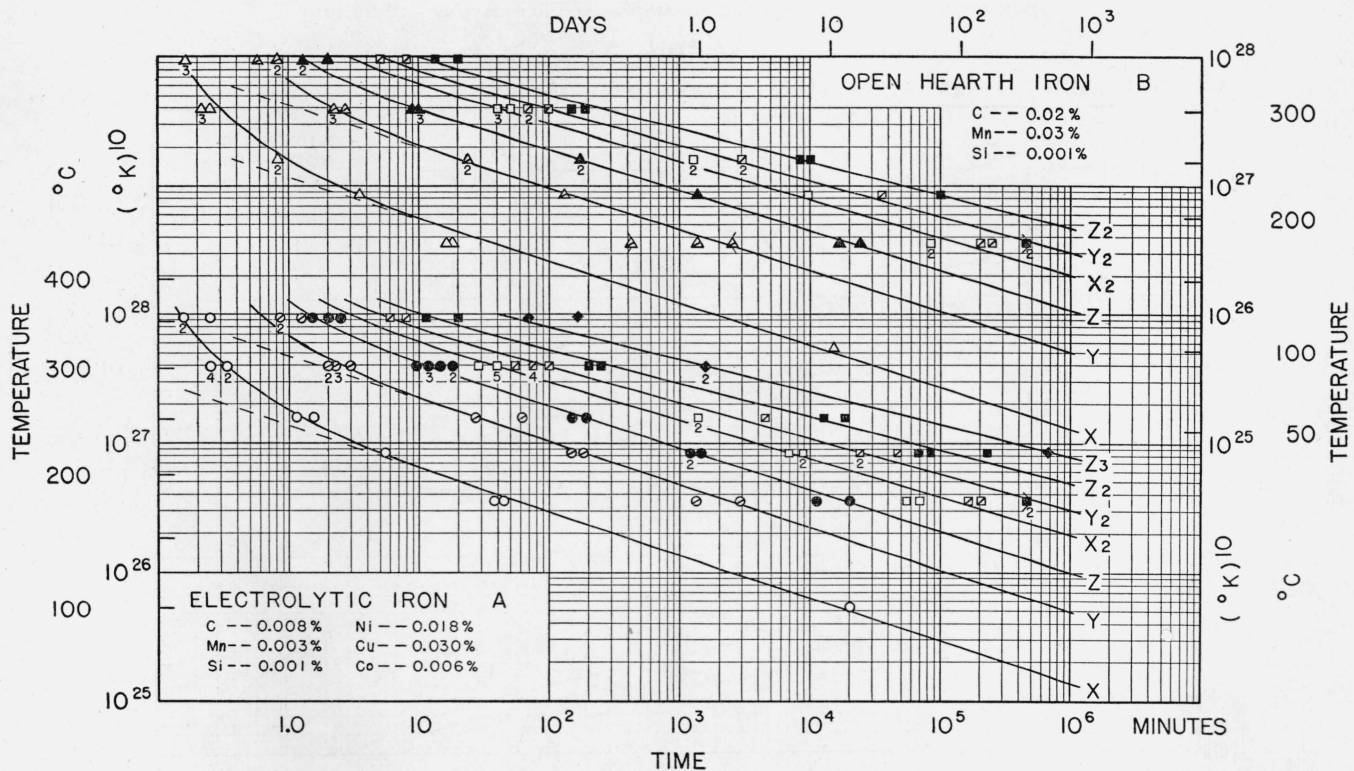


FIGURE 1.—Influence of temperature on the oxidation time of electrolytic iron and open-hearth iron.

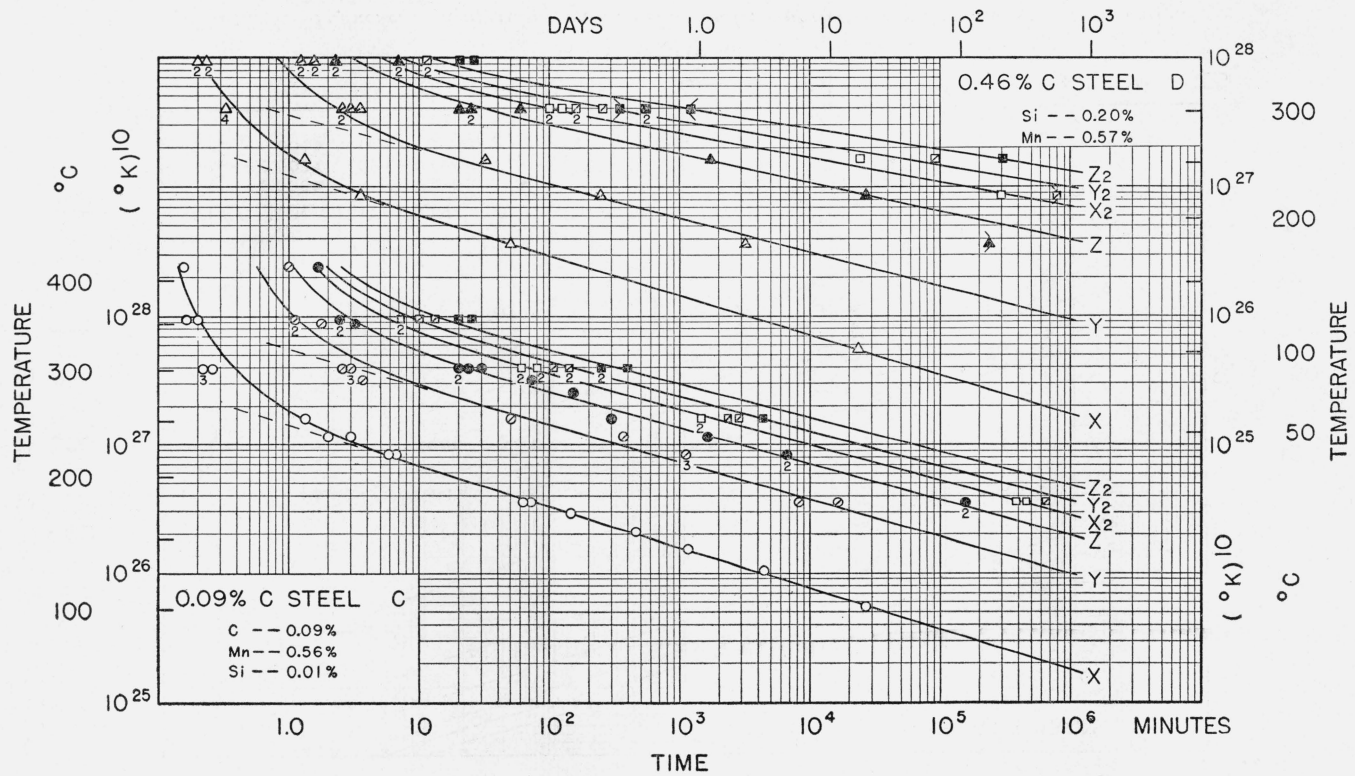


FIGURE 2.—Influence of temperature on the oxidation time of carbon steels.

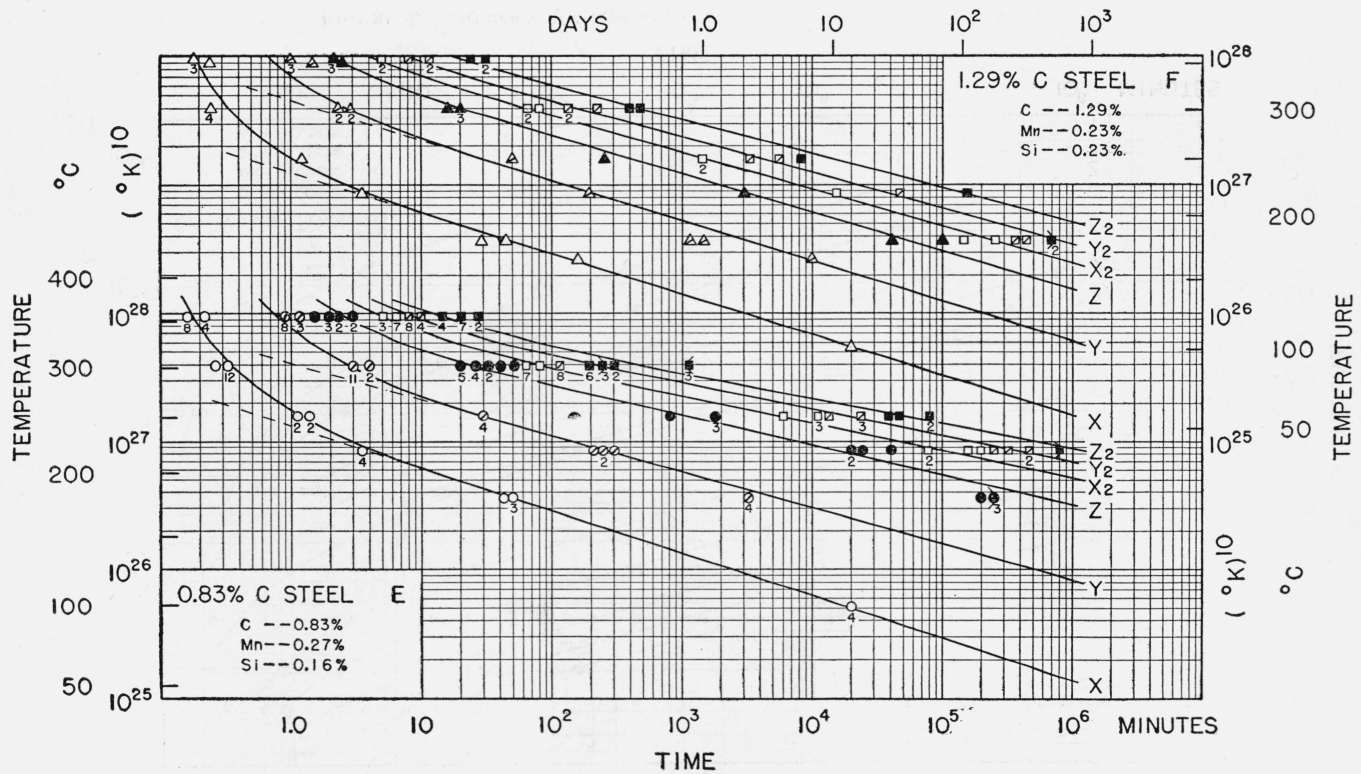


FIGURE 3.—Influence of temperature on the oxidation time of carbon steels.

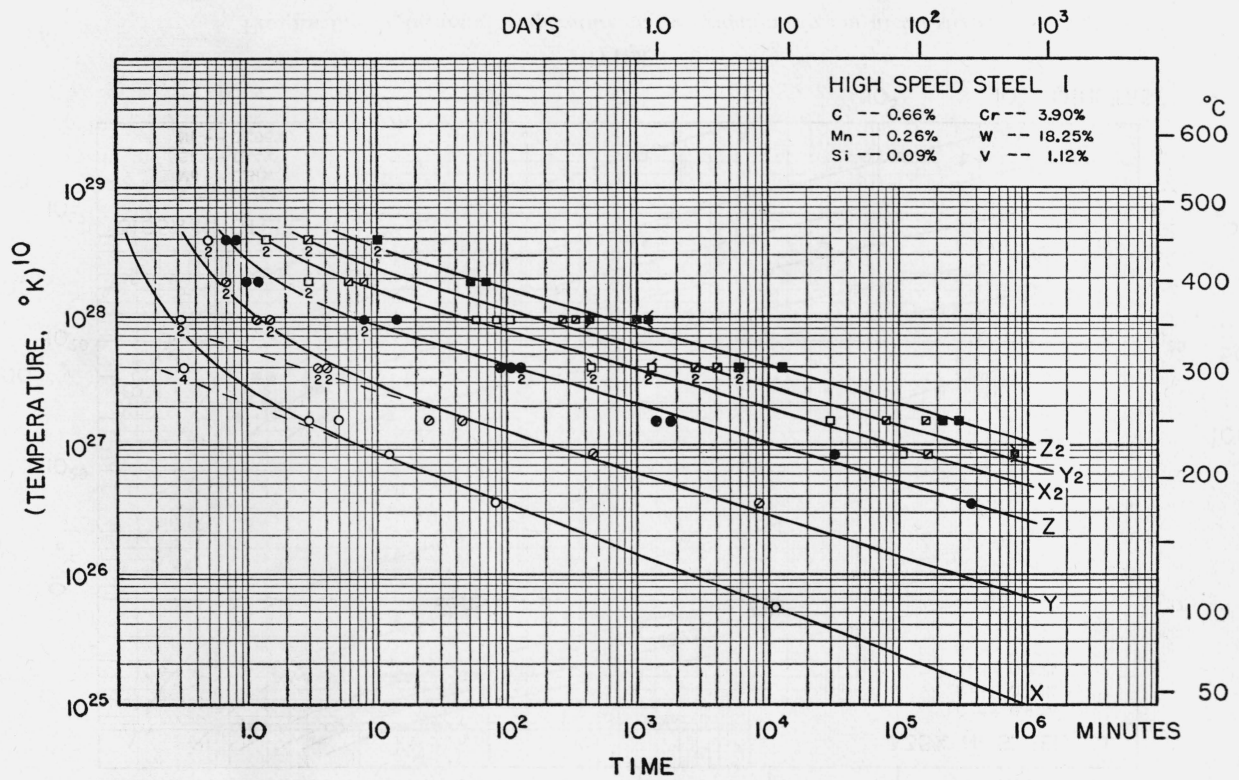


FIGURE 5.—Influence of temperature on the oxidation time of high speed steel.

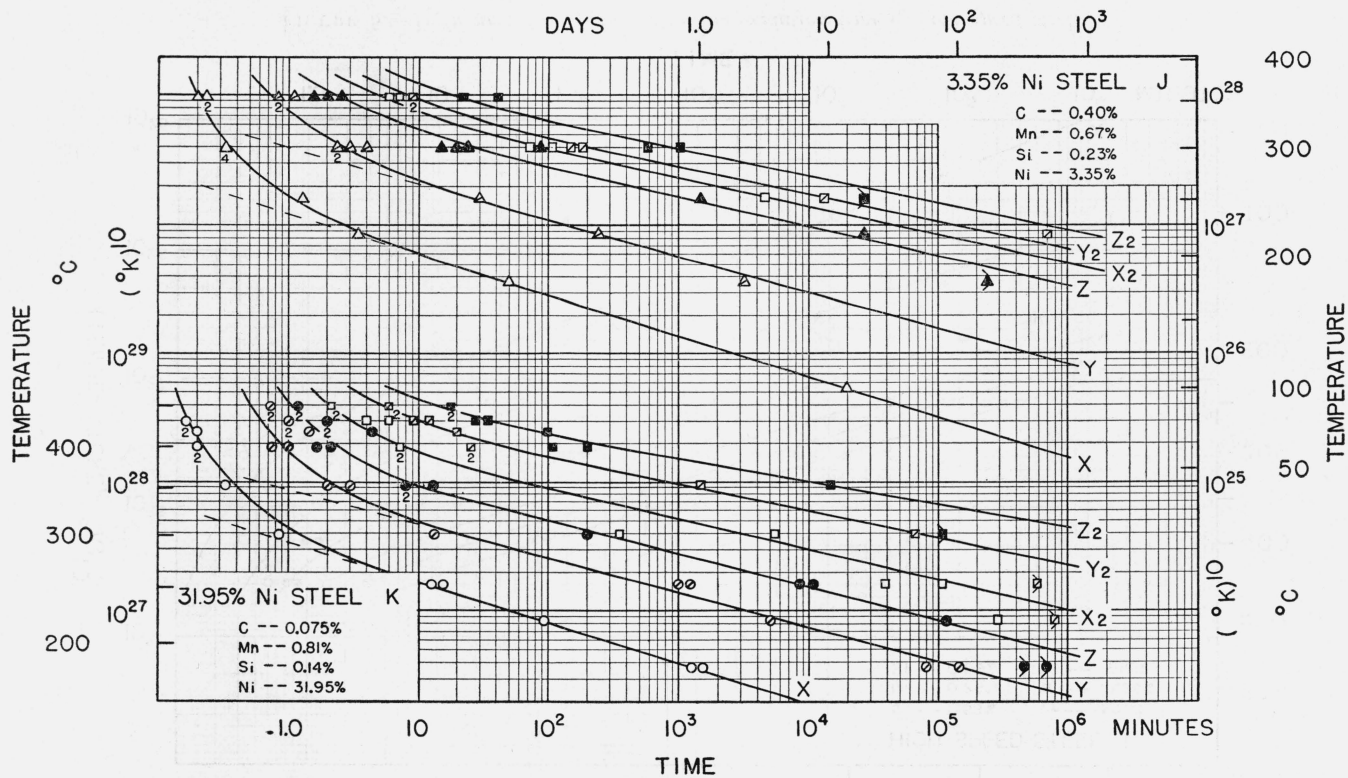


FIGURE 6.—Influence of temperature on the oxidation time of nickel steels.

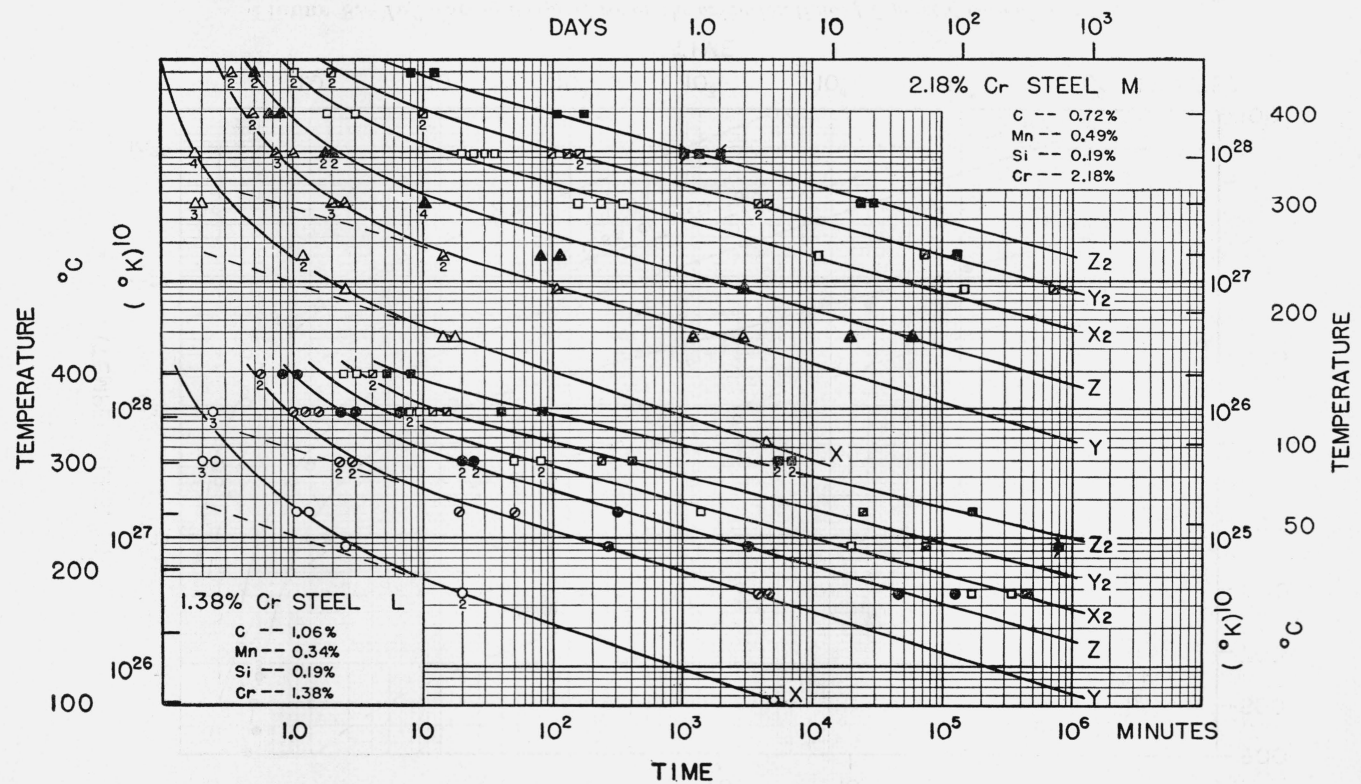


FIGURE 7.—Influence of temperature on the oxidation time of low-chromium steels.

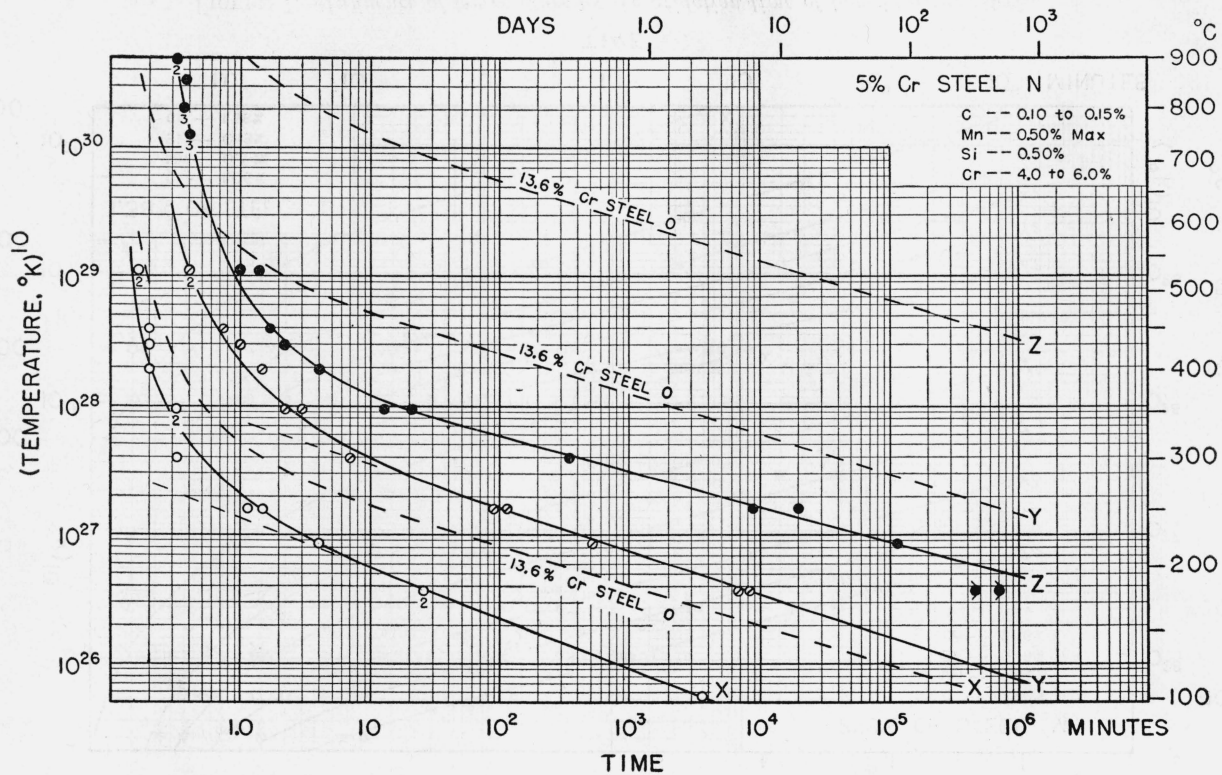


FIGURE 8.—Influence of temperature on the oxidation time of 5 percent chromium steel.

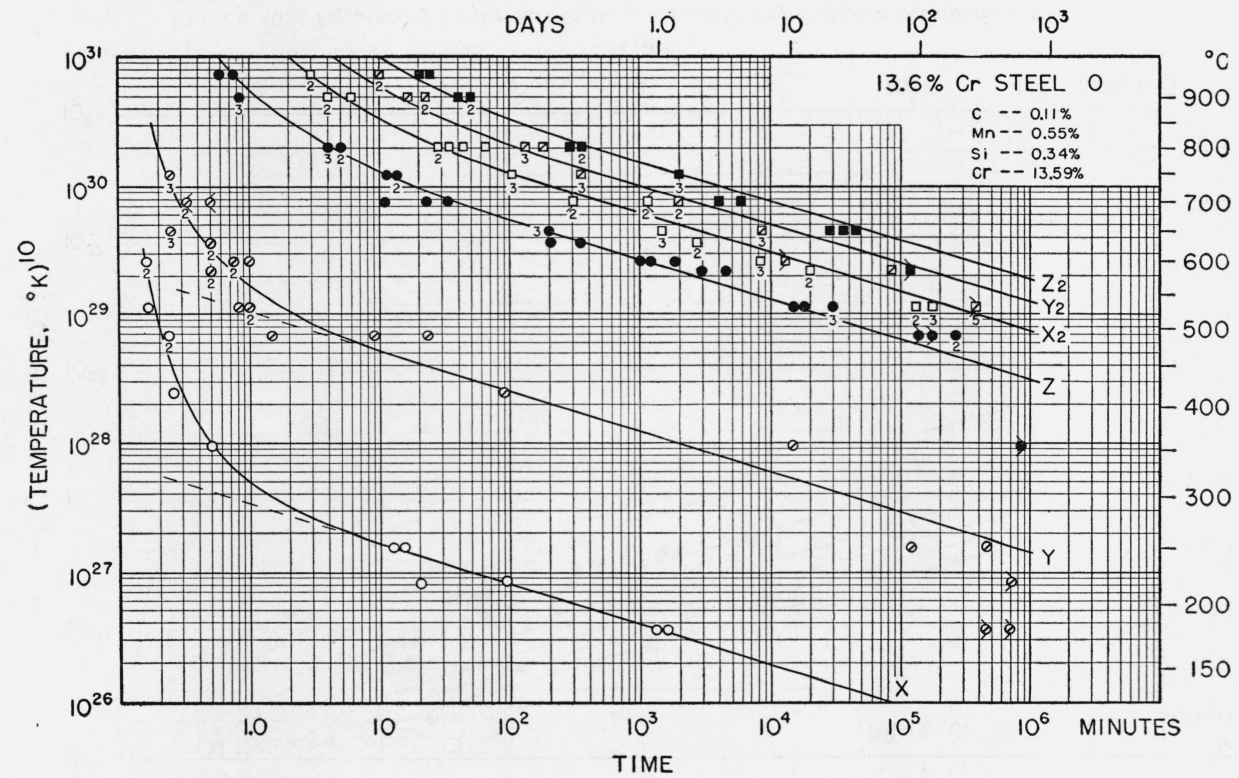


FIGURE 9.—Influence of temperature on the oxidation time of 13.6 percent chromium steel.

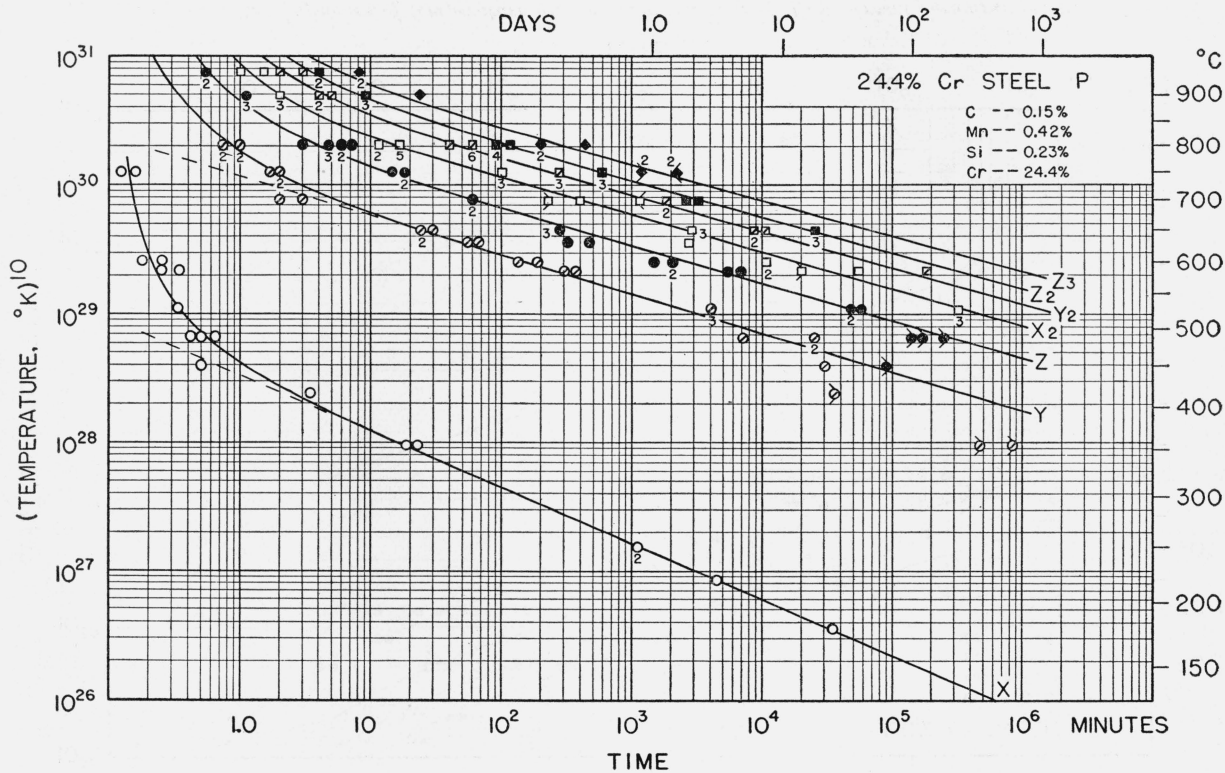


FIGURE 10.—Influence of temperature on the oxidation time of 24.4 percent chromium steel.

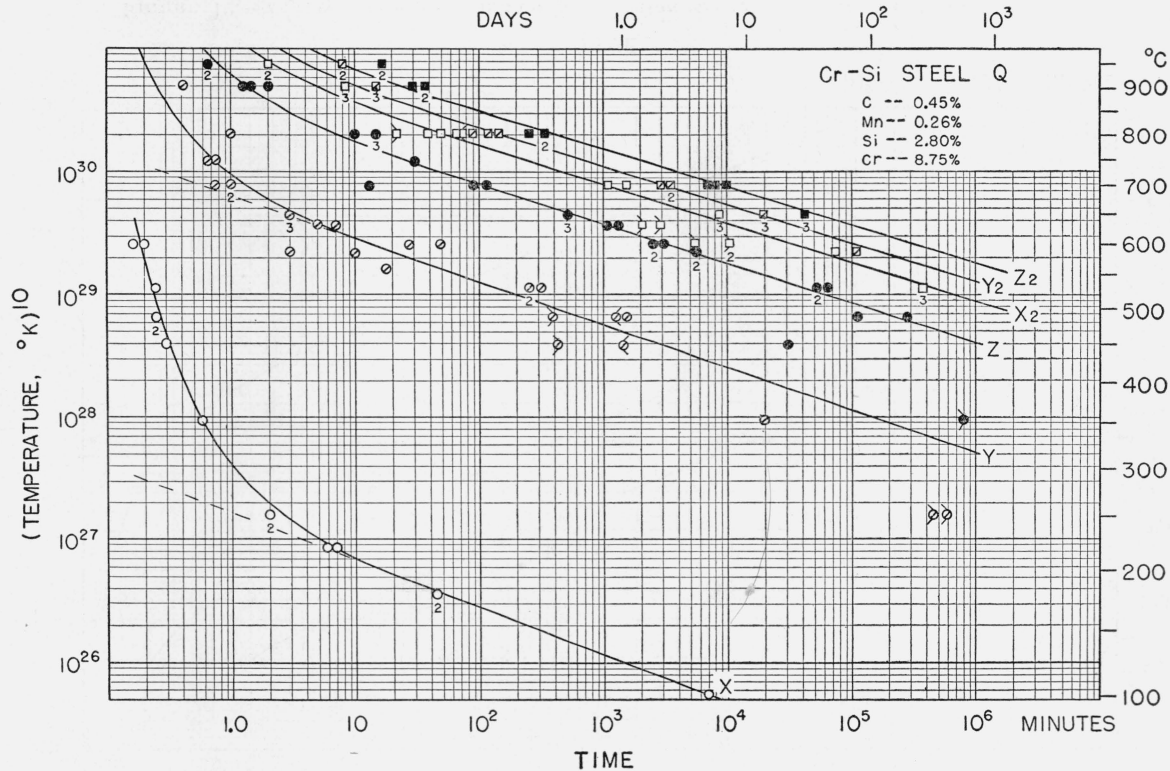


FIGURE 11.—Influence of temperature on the oxidation time of chromium-silicon steel.

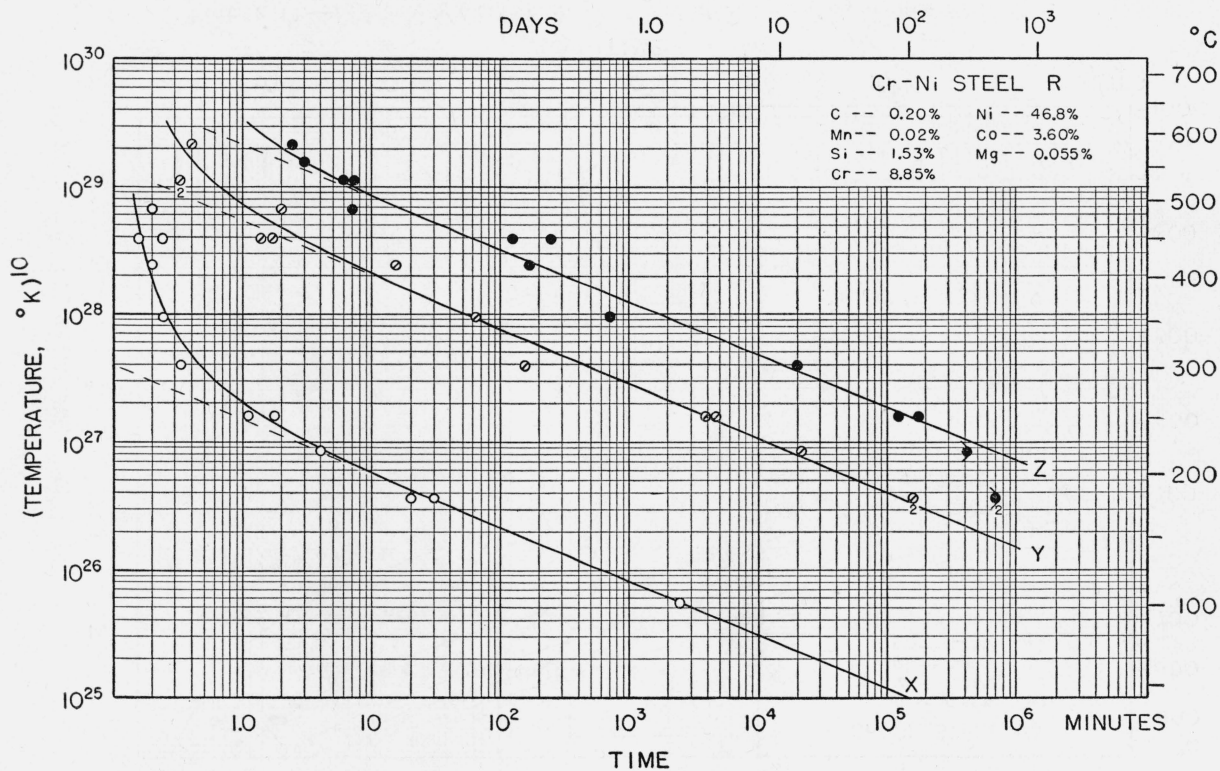


FIGURE 12.—Influence of temperature on the oxidation time of chromium-nickel-cobalt steel.

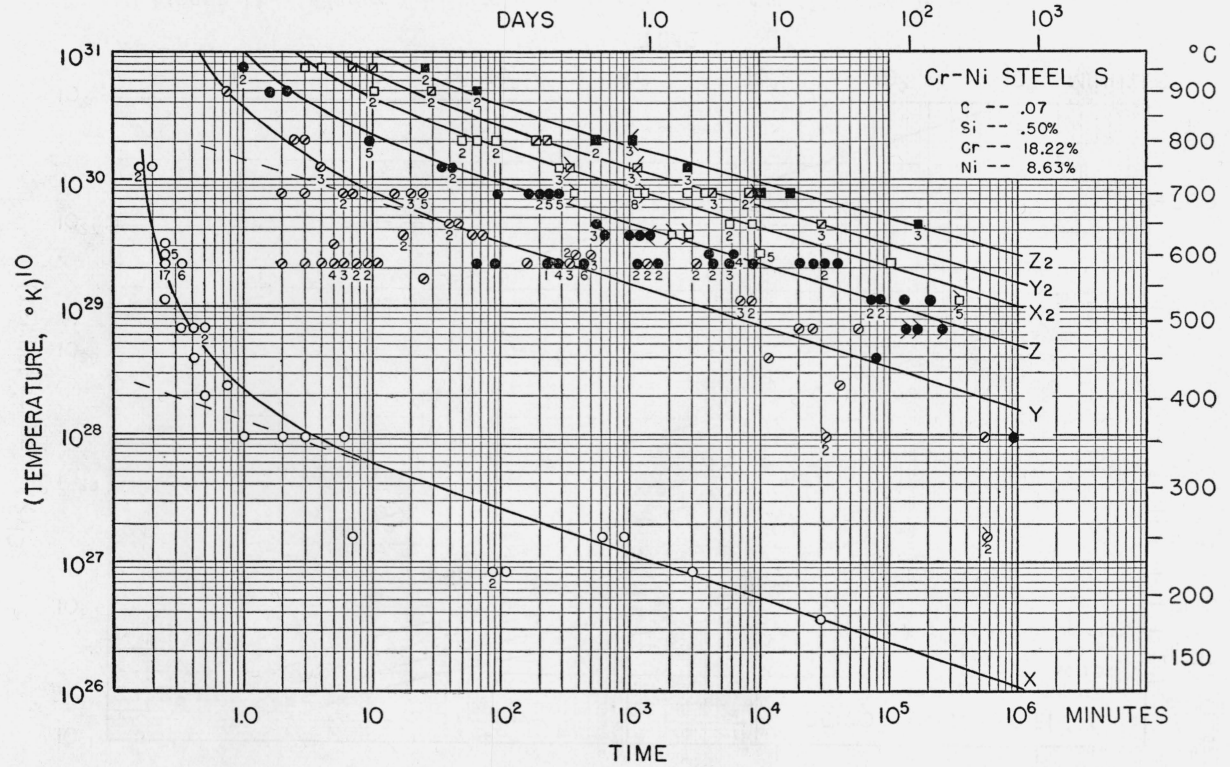


FIGURE 13.—Influence of temperature on the oxidation time of 18:8 chromium-nickel steel.

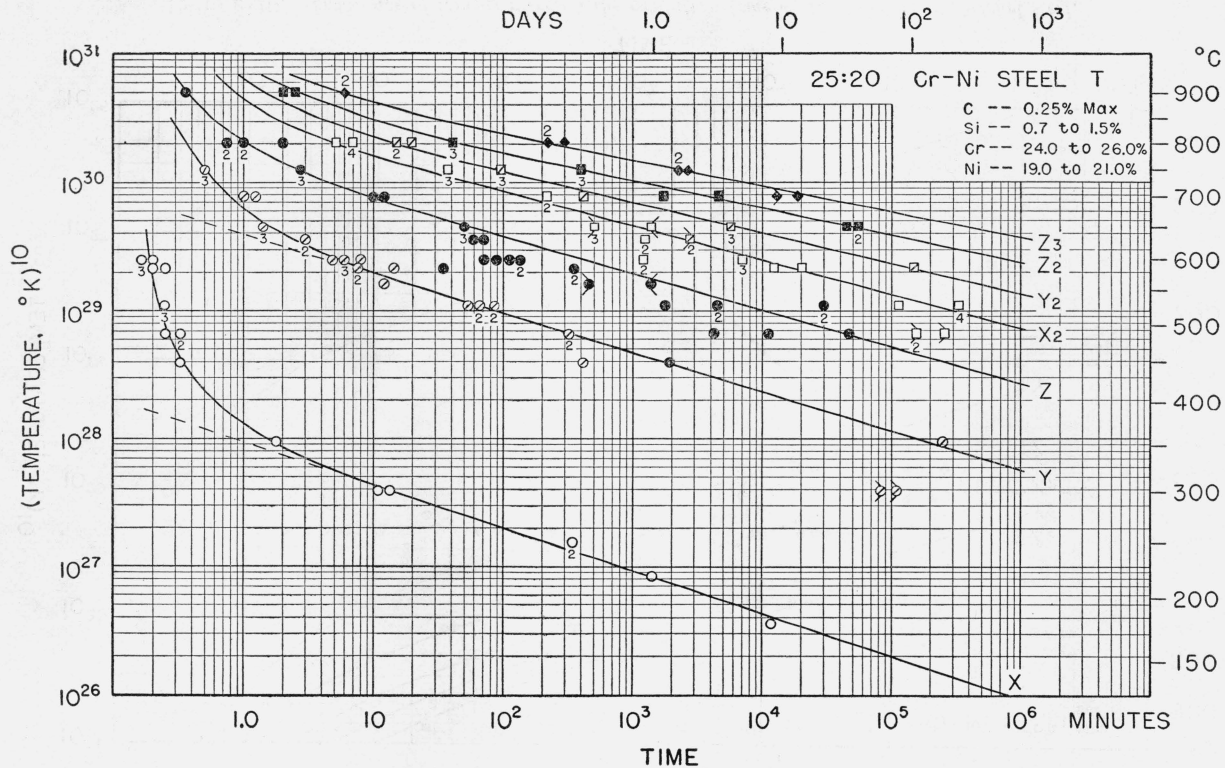


FIGURE 14.—Influence of temperature on the oxidation time of 25:20 chromium-nickel steel.

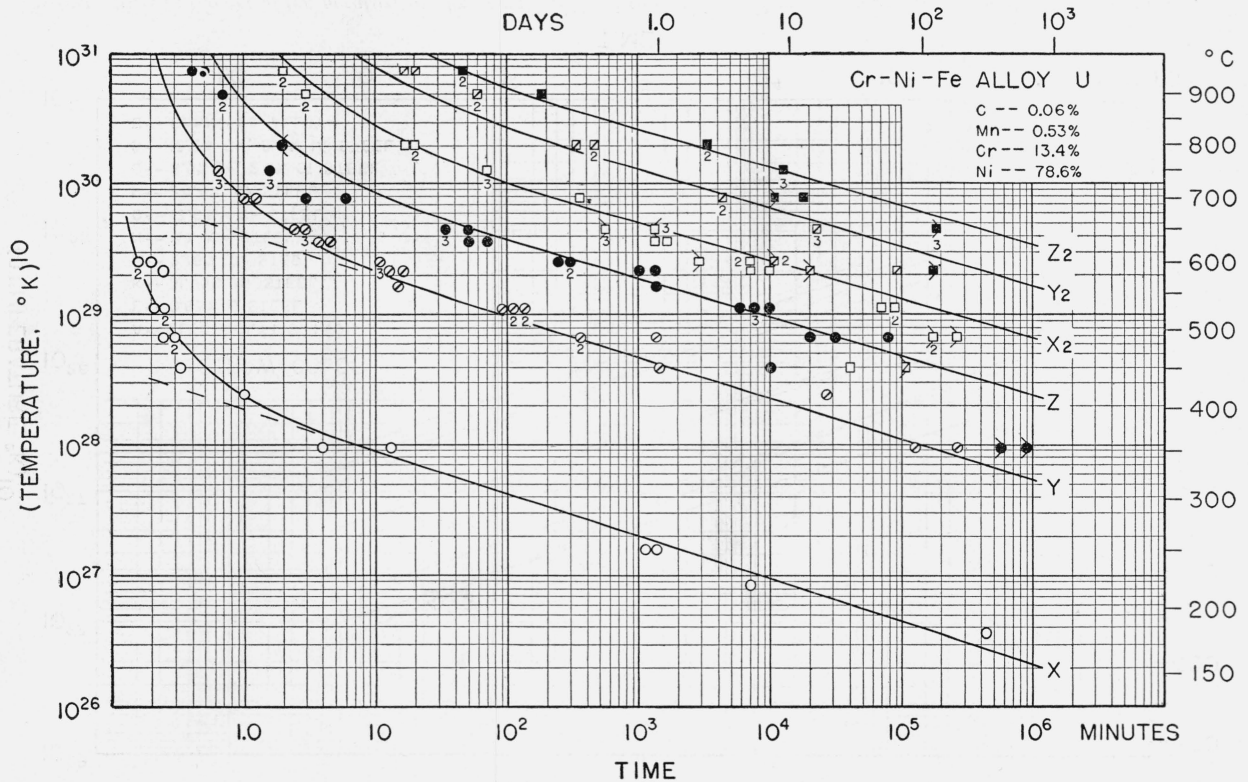


FIGURE 15.—Influence of temperature on the oxidation time of chromium-nickel-iron alloy.

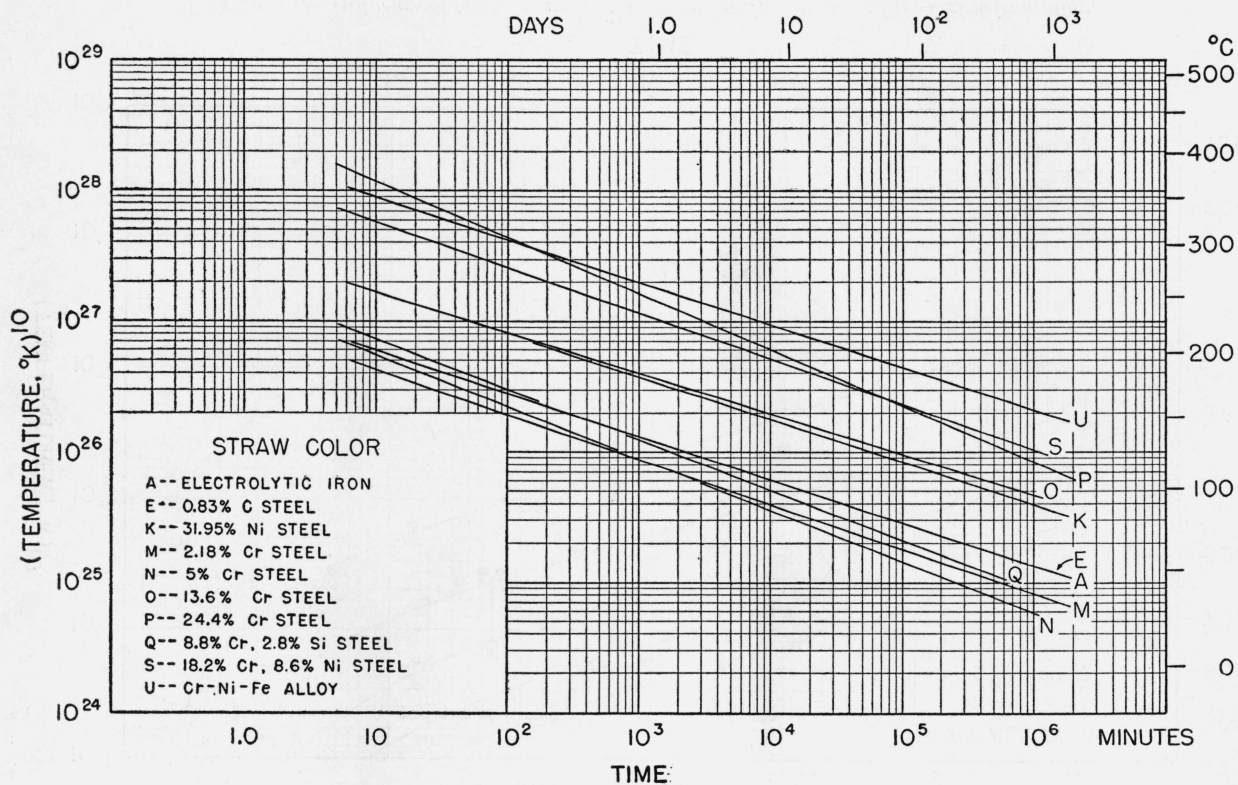


FIGURE 16.—Influence of temperature on the oxidation time; comparison of graphs representing first-order straw color.

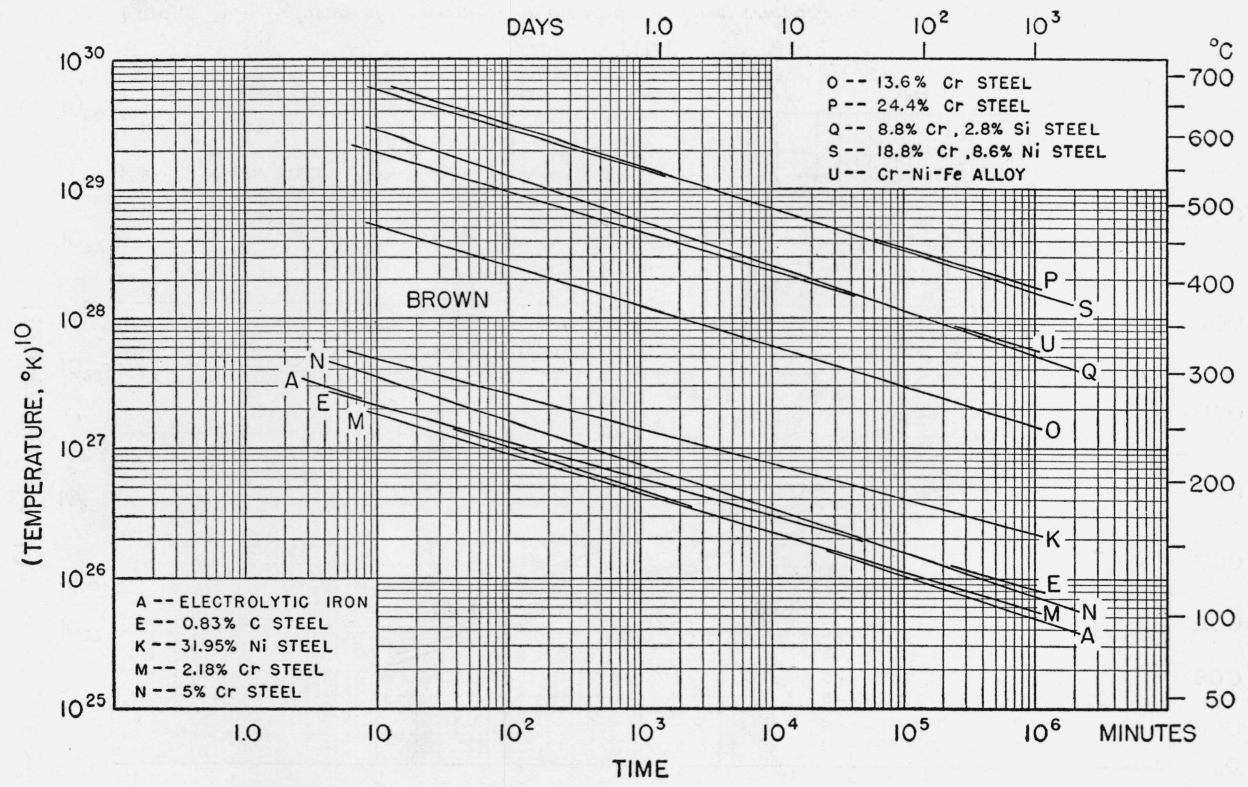


FIGURE 17.—Influence of temperature on the oxidation time; comparison of graphs for first-order brown.

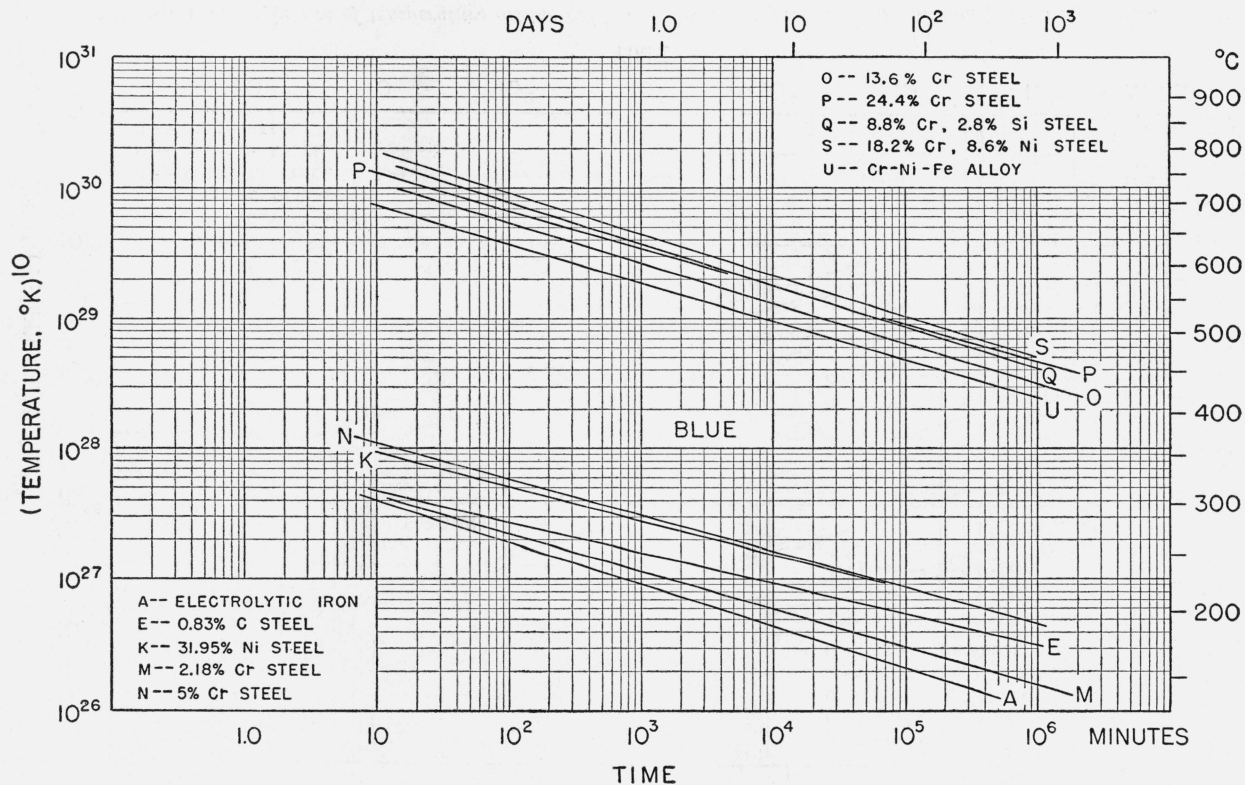


FIGURE 18.—Influence of temperature on the oxidation time; comparison of graphs for first-order blue.

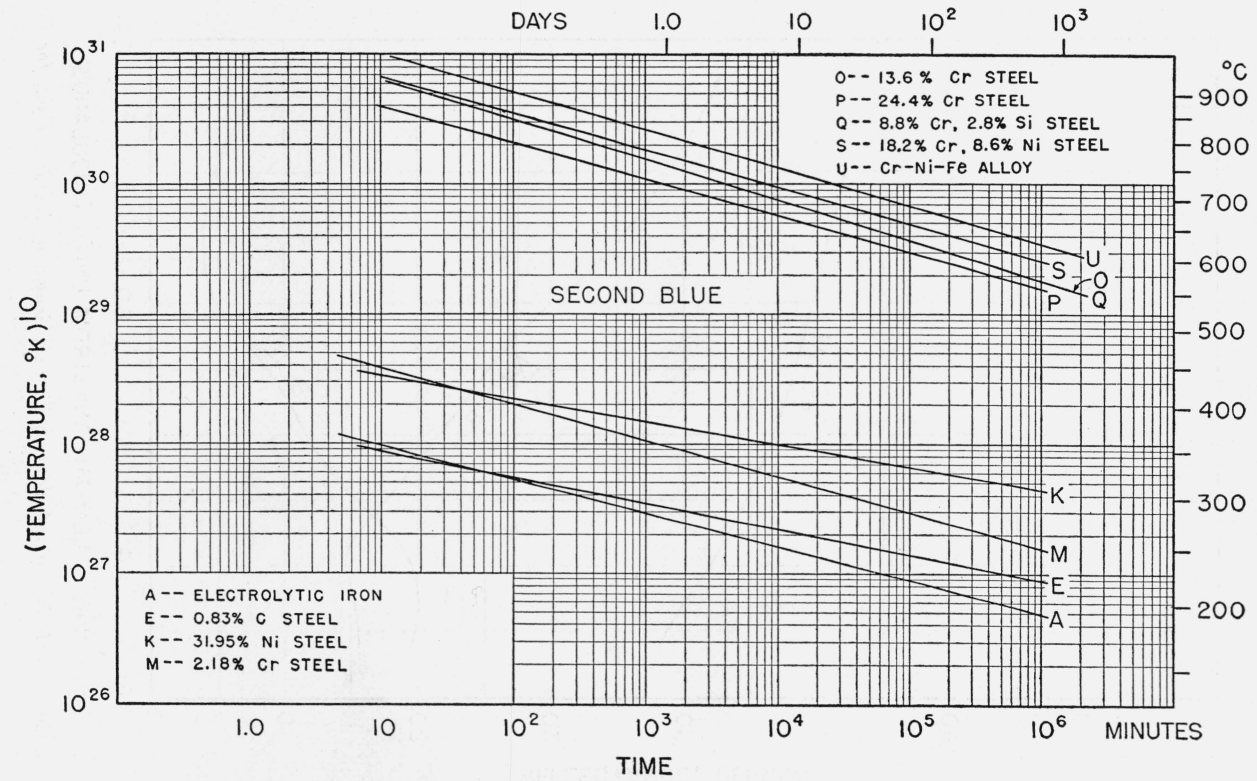


FIGURE 19.—Influence of temperature on the oxidation time; comparison of graphs for second-order blue.

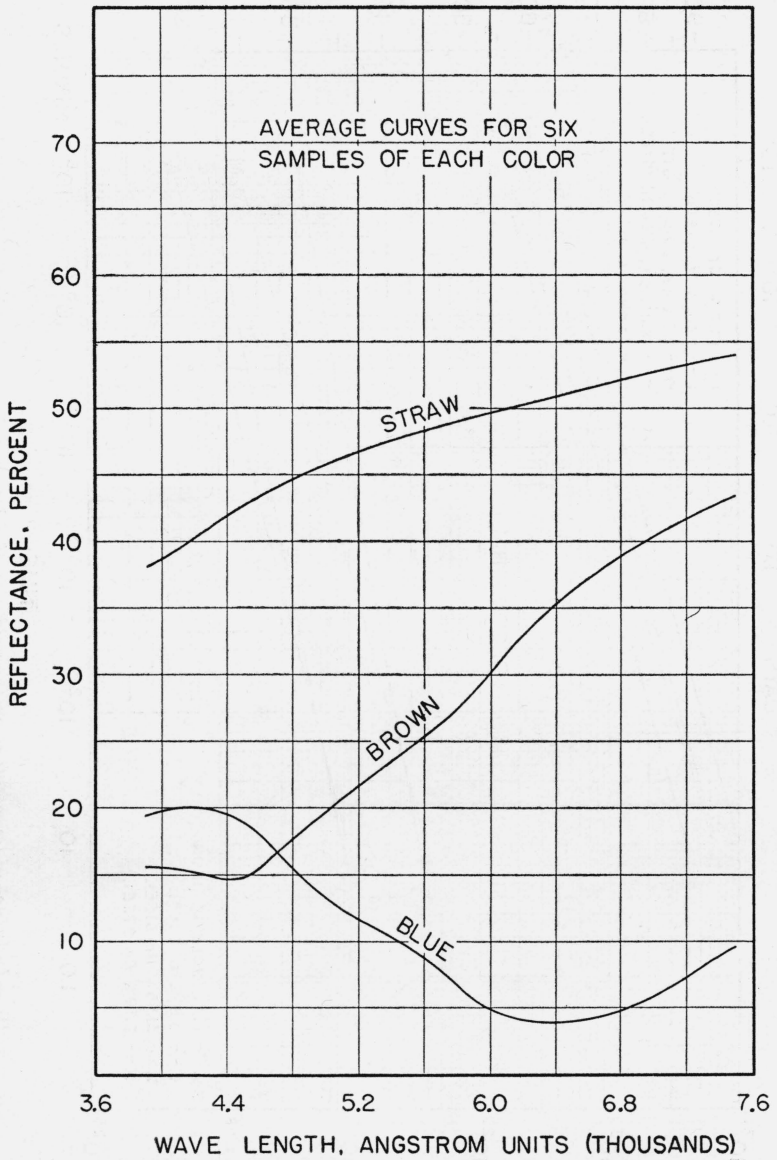


FIGURE 20.—Variation of reflectance with wave length of incident light, for three interference colors.

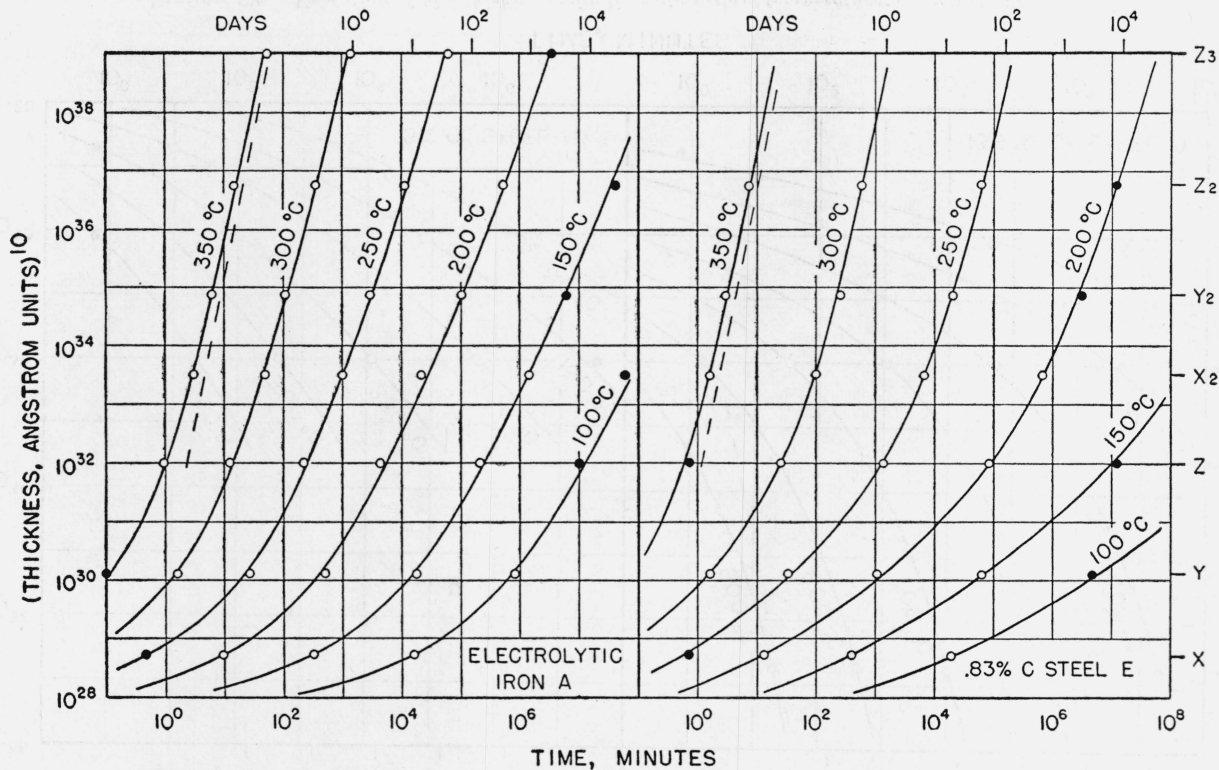


FIGURE 21.—Variation of film thickness with time at constant temperature; electrolytic iron and 0.83-percent carbon steel.

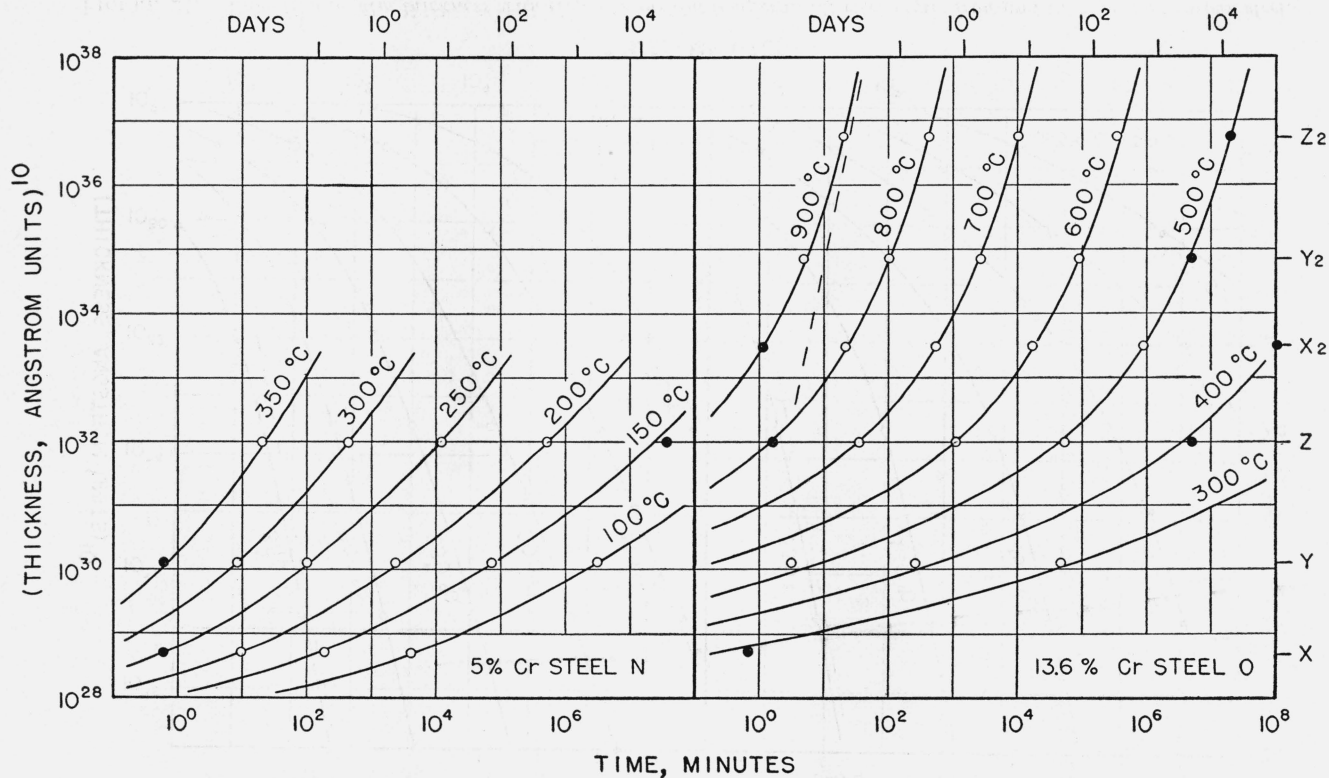


FIGURE 22.—Variation of film thickness with time at constant temperature; chromium steels.

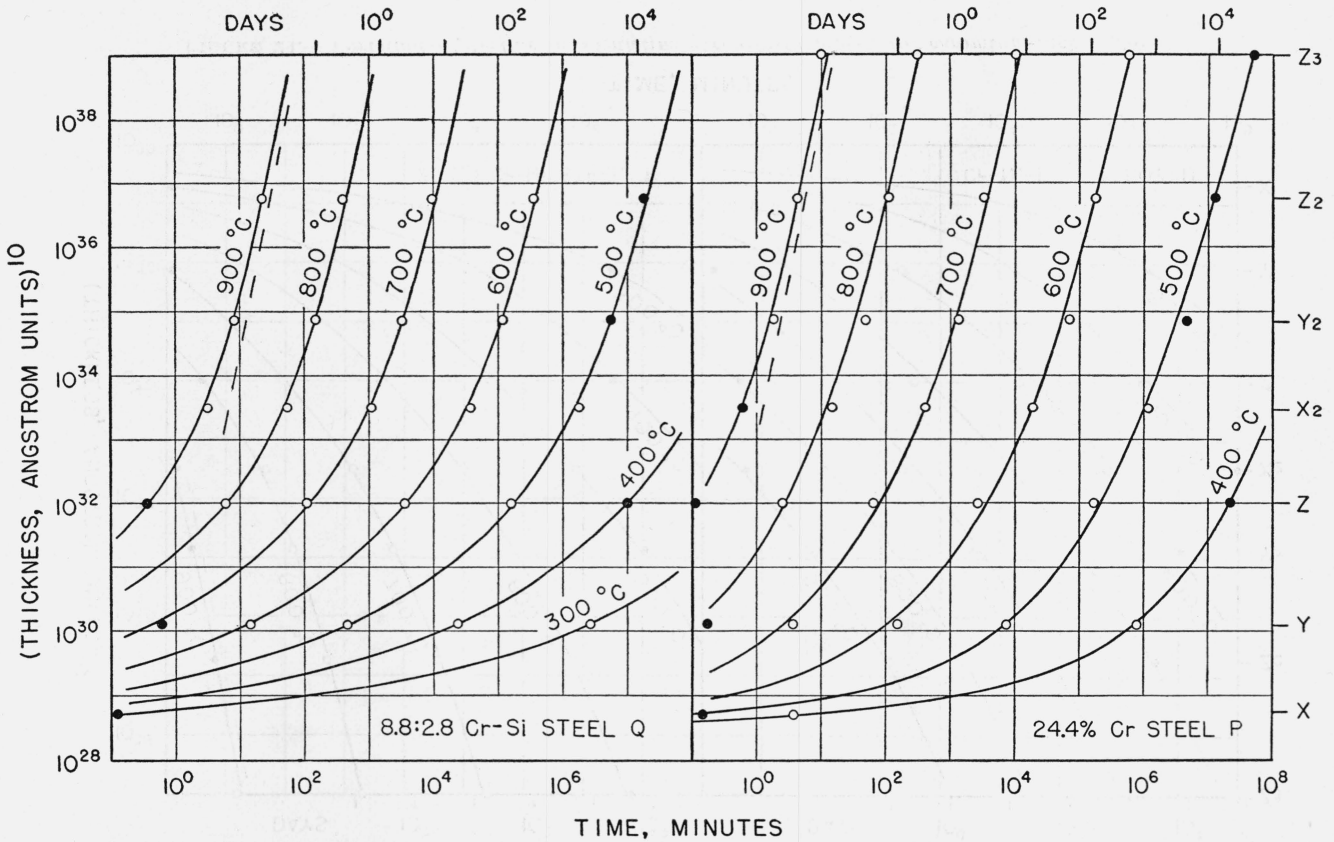


FIGURE 23.—Variation of film thickness with time at constant temperature; chromium-silicon steel and high-chromium steel.

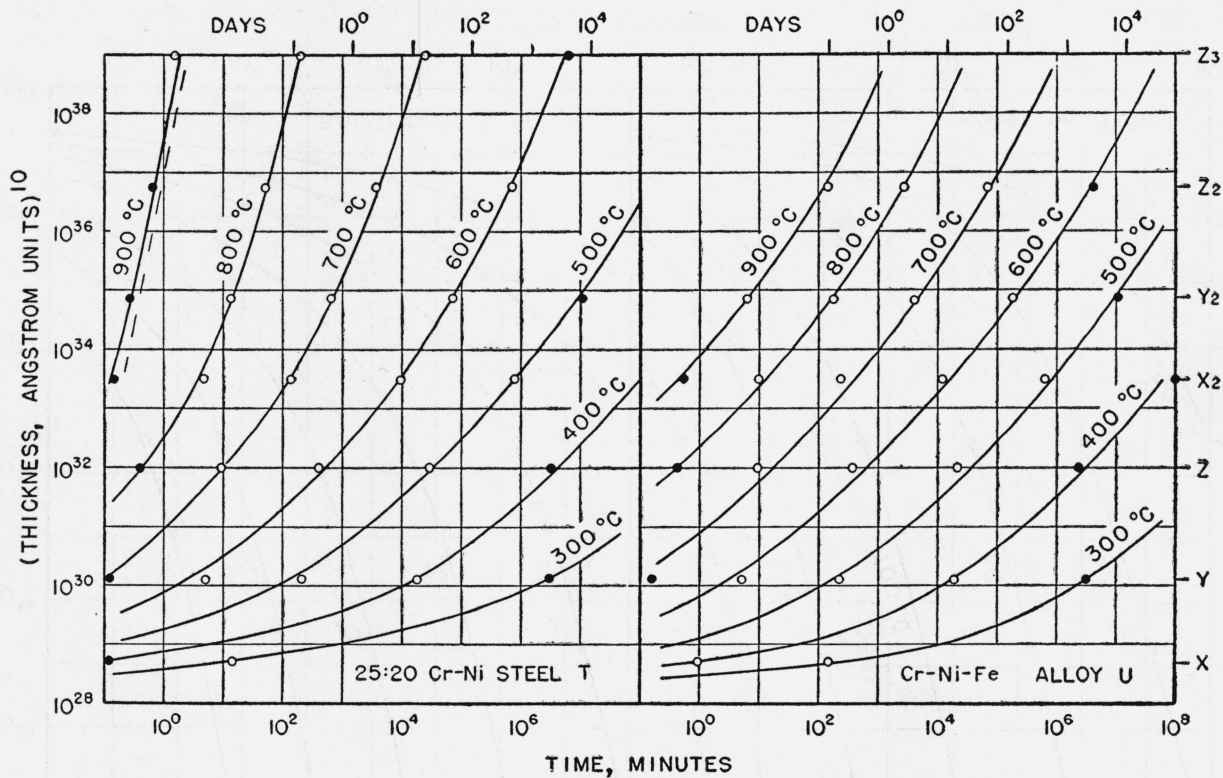


FIGURE 24.—Variation of film thickness with time at constant temperature; chromium-nickel alloys.

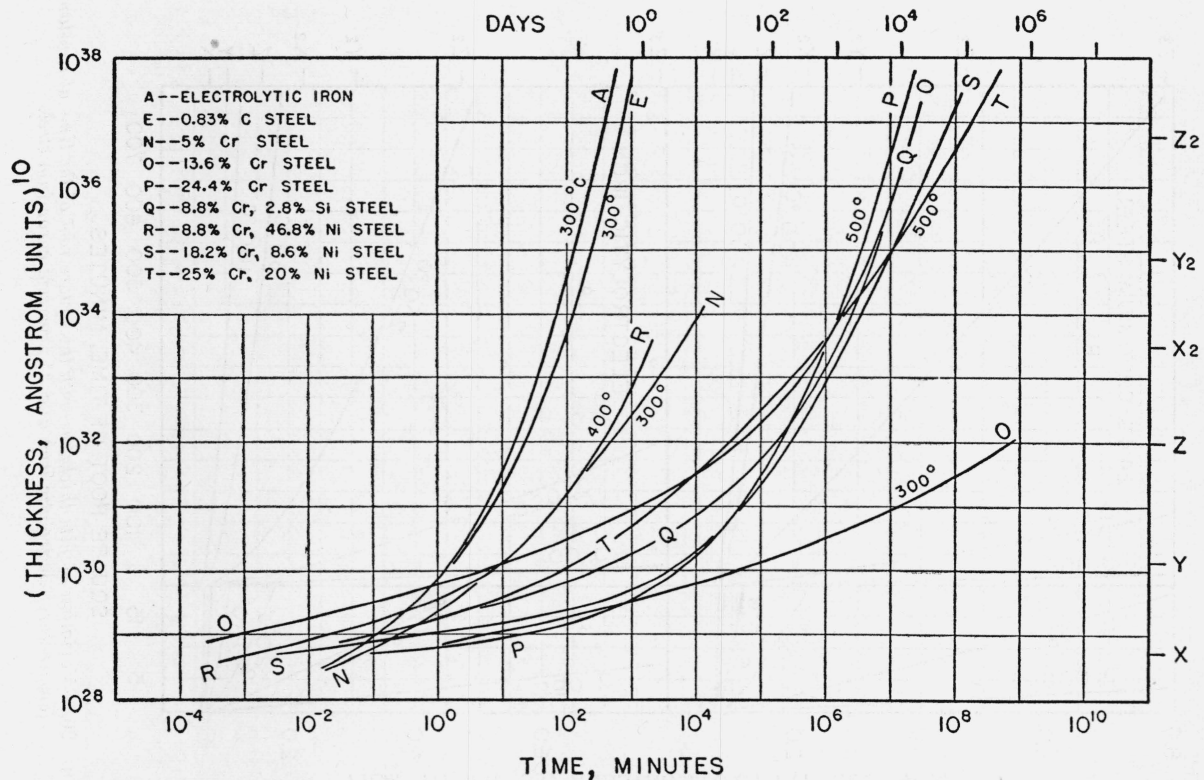


FIGURE 25.—Variation of film thickness with time at constant temperature; comparison of curves for various steels.

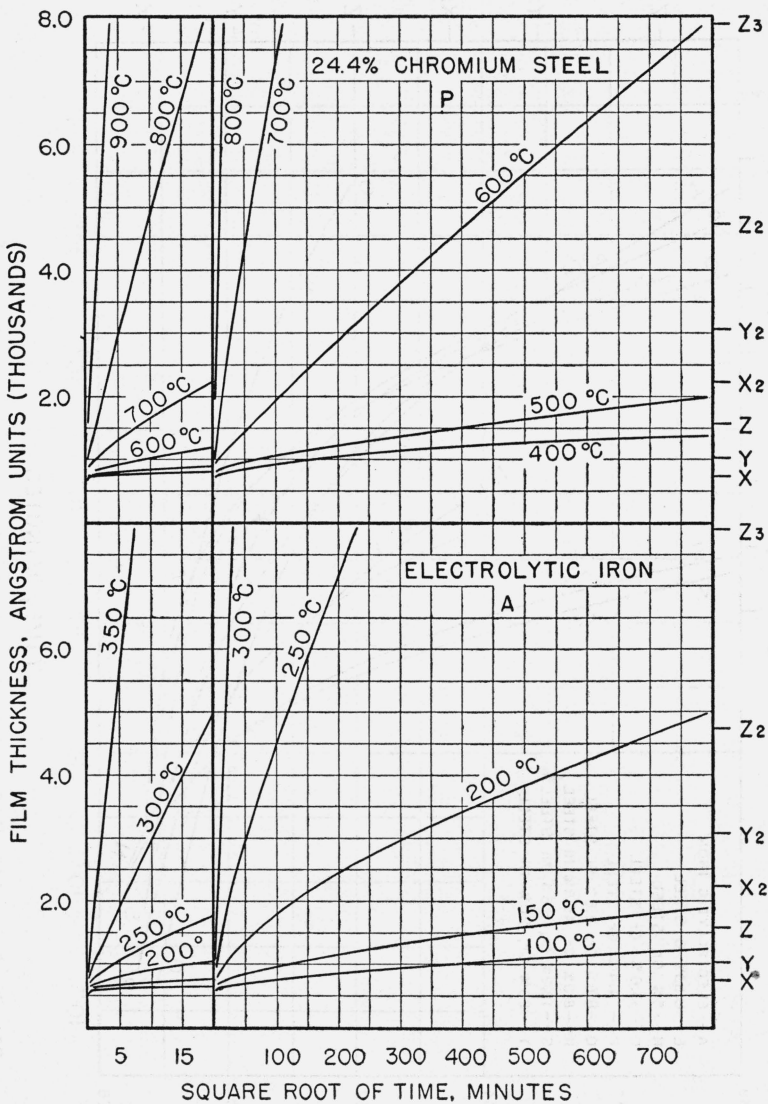


FIGURE 26.—Variation of film thickness with the square root of the time at constant temperature; electrolytic iron and 24.4 percent chromium steel.

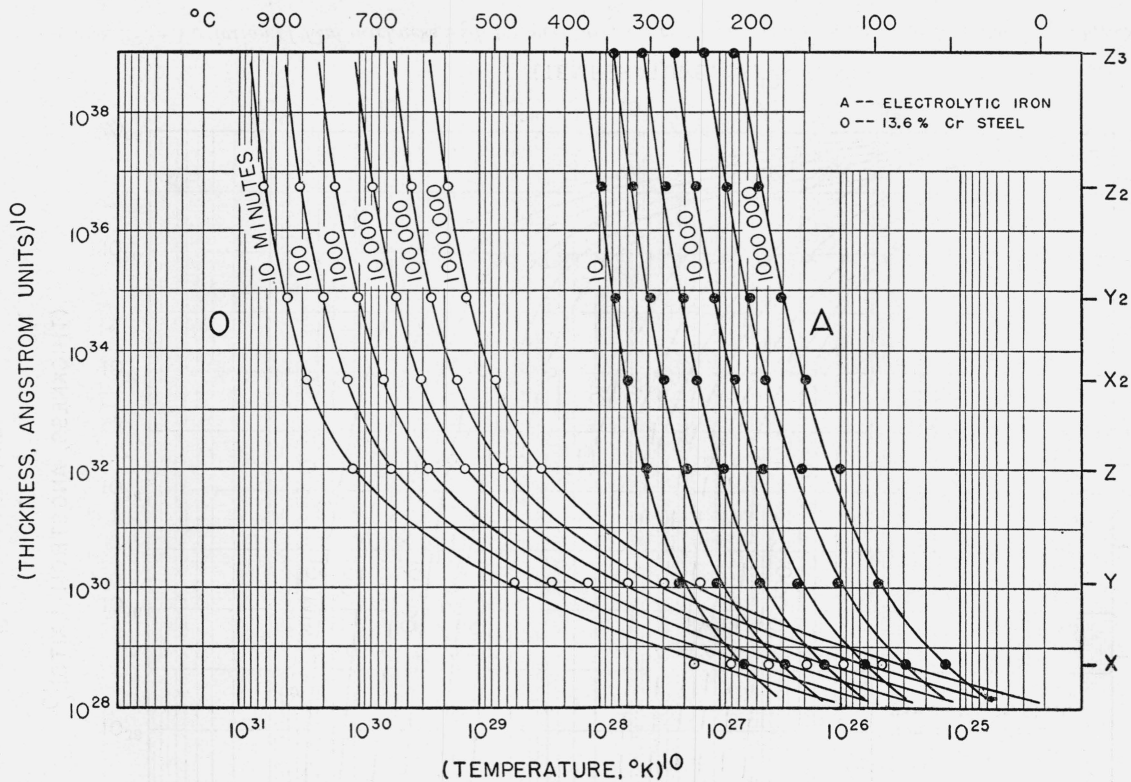


FIGURE 27.—Variation of film thickness with temperature, for constant oxidation time; electrolytic iron and 13.6 percent chromium steel.

